

D6.2 Algorithms for multi-risk analysis of buildings



Funded by
the European Union

D6.2 Algorithms for multi-risk analysis of buildings

Dissemination Level: Public
 Lead Partner: TU Delft
 Due date: 31 December 2024
 Actual submission date: 27 December 2024

PUBLISHED IN THE FRAMEWORK OF

MULTICARE (Horizon Europe grant 101123467)

AUTHORS

Anna Maria Koniari, TU Delft
 Francesco Petrini, UNIROMA1
 Jonathan Ciurlanti, Arup
 Kyujin Kim, TU Delft
 Michele Matteoni, UNIROMA1
 Nicu Ciobotaru, UTBV
 Romulus Costache, UTBV
 Simona Bianchi, TU Delft

REVISION AND HISTORY CHART

VERSION	DATE	EDITORS	COMMENT
V0.1	26 November 2024	Simona Bianchi (TU Delft)	Draft
V0.2	8 December 2024	Anna Maria Koniari (TU Delft)	Draft
V0.3	10 December 2024	Michele Matteoni (UNIROMA1)	Draft
V0.4	12 December 2024	Nicu Ciobotaru, Romulus Costache (UTBV)	Draft
V0.5	16 December 2024	Kyujin Kim (TU Delft)	Draft
V0.6	20 December 2024	Francesco Petrini (UNIROMA1), Jonathan Ciurlanti (Arup)	Review
V1.0	23 December 2024	Simona Bianchi (TU Delft)	Final version

DISCLAIMER

The information in this document is subject to change without notice. Company or product names mentioned in this document may be trademarks or registered trademarks of their respective companies.

All rights reserved

The document is proprietary of the MULTICARE consortium members. No copying or distributing, in any form or by any means, is allowed without the prior written agreement of the owner of the property rights. This document reflects only the authors' view. The European Community is not liable for any use that may be made of the information contained herein. Responsibility for the information and views expressed in the therein lies entirely with the author(s).

Executive Summary

This deliverable details the probabilistic risk assessment methods employed in the MULTICARE project to evaluate social, economic and environmental losses from climate-induced extreme events (heat, flood, wind) and natural disasters (earthquake). These methods integrate uncertainty quantification, probabilistic modelling and numerical simulations to quantify the expected and/or probable maximum consequences. The results feed into the holistic resilience quantification framework described in Deliverable D6.1, enabling a multi-hazard evaluation of building resilience.

Authored by TU Delft, UNIROMA1, Arup and UTBV, the deliverable first outlines key uncertainties in hazard intensity, building characteristics and modeling parameters. These uncertainties are systematically integrated into probabilistic risk assessment methods which enable to quantify building-level losses. These losses are considered into a multi-criteria decision making approach to compute a unified resilience score for buildings. The methodology for calculating this score will be provided as Python scripts openly accessible via the MULTICARE GitHub repository (Deliverables D6.2 and D6.3). This score will be integrated into a digital tool specifically designed to support early-stage design or retrofit selection. The tool will facilitate the resilience quantification for the buildings in the demo sites, as preliminarily outlined in the appendix of this document.

Table of contents

1. Introduction	8
1.1. MULTICARE project	8
1.2. Algorithms for multi-risk analysis of buildings	10
1.2.1 Objectives and method	11
1.2.2 Relation to other activities	11
2. Uncertainty in risk assessment	13
2.1 Hazard uncertainties	13
2.2 Building uncertainties	18
2.3 Modelling uncertainties	25
2.4 Summary	28
3. Risk assessment of buildings	29
3.1. Seismic risk	29
3.2. Wind risk	31
3.3. Flood risk	32
3.4. Heat risk	33
4. Resilience quantification	36
5. Conclusions	39
6. References	40
Appendix A – Preliminary results	40

LIST OF FIGURES

Figure 1. Consequences associated with each analyzed hazard	10
Figure 2. Extract from Table 5-6 of FEMA P-58 (2018): dispersions for record-to-record variability for use with simplified analysis (where S represents the building strength, assessed from its weight W , the 5% damped spectral acceleration at the building's fundamental period $S_a(T_1)$, and the estimated yield strength of the building in its first mode response V_{y1})	14
Figure 3. Annual dry bulb temperature values produced through morphing of TMY values according to different SSP scenarios for year 2050 (EC-Earth3 climate model). Morphing was performed using the future weather generator from (Rodrigues, Fernandes, & Carvalho, 2023).	16
Figure 4. Example of cumulative probability distribution for a scenario earthquake (FEMA P-58 2018)	17
Figure 5. Stochasticity in age factor (AF) and uninsulated area ratio (UAR) of the building envelope as described in (Liu et al., 2022)	21
Figure 6. Sampling across and within building stocks (Van Hove et al., 2023)	22
Figure 7. Uncertainty related to consequence functions based on component quantity (FEMA P-58 2018)	24

Figure 8. Normative Quantities for Multi-Unit Residential Occupancies – Extract from Table F-5 of FEMA P-58.....	26
Figure 9. Uncertainty sources in risk modelling	28
Figure 10. PEER framework for loss modelling	30
Figure 11. Fault tree for a service disruption given the occurrence of nonstructural damage (Merhi et al., 2025)	32
Figure 12. Loss modelling framework proposed by Nofal et al. (2020)	33
Figure 13. Thermal fragility curves derivation process (Kim et al, 2024)	34
Figure 14. Derivation of seismic resilience curves.....	37

LIST OF TABLES

Table 1. Consortium	9
Table 2. Relation to other WPs.....	12
Table 3. Uncertainty studies on inherent variability and measurement errors in material properties	19
Table 4. Studies applying fixed yearly rates to express the deterioration of thermal performance because of ageing	20
Table 5. Studies examining the effect of ageing on component thermal resistance / transmittance	21
Table 6. Variability in infiltration rate	22
Table 7. Key uncertainties associated with construction detailing	23
Table 8. Uncertainties in occupant behavior.....	24
Table 9. Dispersion values for quality of the analytical model	27
Table 10. Resilience indicators derived from loss modelling.....	36

GLOSSARY

ACRONYM	FULL NAME
CFD	Computational Fluid Dynamics
EAL	Expected Annual Loss
GCM	Global Climate Model
KPI	Key Performance Indicator
MCDM	Multi-Criteria Decision-Making
RRL	Resilience Readiness Levels
SSP	Shared Socio-economic Pathway
TMY	Typical Meteorological Year
WP	Work Package

1. Introduction

1.1. MULTICARE project

The built environment is ill-prepared for more frequent and increasingly intense climate-related extreme events. The current building stock is particularly vulnerable because it has limited or no capacity to adapt and recover from extreme events thereby leading to building failures that cause severe socio-economic losses and adversely affecting the health and wellbeing of people. Recent scientific and technological advances in the construction industry provide timely solutions for improving the resilience for specific single hazards (e.g. flood hazard or seismic hazard), but they are often not cost effective, rarely eco-friendly and nearly never address the multiple hazards present in many locations. This is hardly surprising because there is neither a clearly defined framework for quantifying the whole-life socio-economic-environmental impacts of extreme natural events nor tools for assessing the holistic climate resilience of buildings. Consequently, it is currently very challenging to develop/select optimal solutions for real-world multi-hazard scenarios.

MULTICARE will address this challenge directly by developing new multi-criteria decision-support frameworks and providing plug & play technological and digital solutions for improving the resilience of the built environment in a cost-effective, reliable and sustainable manner. The technological solutions consist of multi-functional low-carbon resilient technologies embedded in modular and prefabricated construction for the next generation of high performance and smart buildings, characterized by enhanced safety, energy efficiency, environmental-sustainability, improved quality of life, circularity, and scalability for a broad range of natural events and end-user. The plug & play technologies will be applied to either new multi-story buildings or existing structures by means of low-invasive external interventions. The digital solutions consist of a suite of multi-disciplinary digital services and tools for performing multi-hazard resilience assessment, design, operation and management across multiple scales (material, component, building, neighborhood/city). The new digital tools will enable stakeholders to make informed decisions in the selection of materials/solutions, including for heritage buildings, and support resilient supply chains. The effectiveness of the MULTICARE solutions will be demonstrated through large-scale pilots (3 buildings, 4 neighborhoods/district) in three different European countries carefully selected for their diverse local environmental, social and economic conditions (Italy, Netherlands, Romania). Banks and institutional investors will be engaged to better understand the financial risk reduction value of resilience and update existing and future “green finance” mechanisms that will help to leverage the project results. A user-center, inclusive and participatory approach will be consistently implemented throughout the project to engage citizens and extend the durability of MULTICARE impact.

To achieve these ambitious goals, MULTICARE brings together a unique interdisciplinary Consortium of 21 partners (**Table 1**) from 6 different EU countries with strong R&D and practical expertise, who are either established leaders in their sector or agile SMEs in emerging fields. Altogether the Consortium members span across the whole technical and

value chain required for developing and implementing solutions in terms of design, digitization, manufacturing, construction and monitoring of resilient and sustainable buildings. The Consortium also includes partners with experience in social sciences, user engagement, and training to ensure the success and widespread application of new technologies in local communities. The Consortium will also support clustering activities with other relevant research projects to share knowledge and raise public awareness of building resilience. An international outreach and cooperation strategy will also be implemented to tackle the project challenges.

Table 1. Consortium

Number	Role	Short Name	Legal Name	Country
1	CO	TU Delft	TECHNISCHE UNIVERSITEIT DELFT	NL
2	BEN	PFE	PRIEDEMANN FASSADENBERATUNG GMBH	DE
3	BEN	IES R&D	IES R&D	IE
4	BEN	INCDFP	INSTITUTUL NATIONAL DE CERCETARE-DEZVOLTARE PENTRU FIZICA PAMANTULUI	RO
5	BEN	UNIROMA1	UNIVERSITA DEGLI STUDI DI ROMA LA SAPIENZA	IT
6	BEN	XLD	X-LAM DOLOMITI SRL	IT
7	BEN	STRESS	SVILUPPO TECNOLOGIE E RICERCA PER L'EDILIZIA SISMICAMENTE SICURA ED ECOSOSTENIBILE SCARL	IT
7.1	AE	UNINA	UNIVERSITA DEGLI STUDI DI NAPOLI FEDERICO II	IT
8	BEN	AMS Institute	STICHTING AMSTERDAM INSTITUTE FORADVANCED METROPOLITAN SOLUTIONS(AMS)	NL
9	BEN	PMB	MUNICIPIUL BUCURESTI	RO
10	BEN	ASM	ASM - CENTRUM BADAN I ANALIZ RYNKUSPOLKA Z OGRANICZONA ODPOWIEDZIALNOSCIA	PL
11	BEN	RoGBC	ASOCIATIA ROMANIA GREEN BUILDING COUNCIL	RO
12	BEN	RINA-C	RINA CONSULTING SPA	IT
13	BEN	UTBV	UNIVERSITATEA TRANSILVANIA DIN BRASOV	RO
14	BEN	ACER	AGENZIA CAMPANA PER L EDILIZIA RESIDENZIALE	IT
15	BEN	Boom	BOOM BUILDS B.V.	NL
16	BEN	OMRT	OMRT BV	NL
17	BEN	ROTHO BLAAS SRL	ROTHO BLAAS SRL	IT
18	BEN	ARUP	ARUP BV	NL
19	BEN	Tecuci	MUNICIPIUL TECUCI	RO
20	BEN	Hölscher	DIPL.-ING. HPLSCHER GMBH & CO.KG	DE

1.2. Algorithms for multi-risk analysis of buildings

This deliverable describes the probabilistic risk assessment methods employed to evaluate social (e.g., casualties), economic (direct and indirect costs), and environmental (carbon emissions) losses resulting from future climate-induced extreme events (heatwaves, floods and wind-related) and natural disasters such as earthquakes. These overall consequences, summarized in **Figure 1**, are integral to the impact assessment of the MULTICARE solutions, as defined in the project concept described in Deliverable D4.4, and considered in the holistic resilience quantification of buildings, as detailed in Deliverable D6.1.

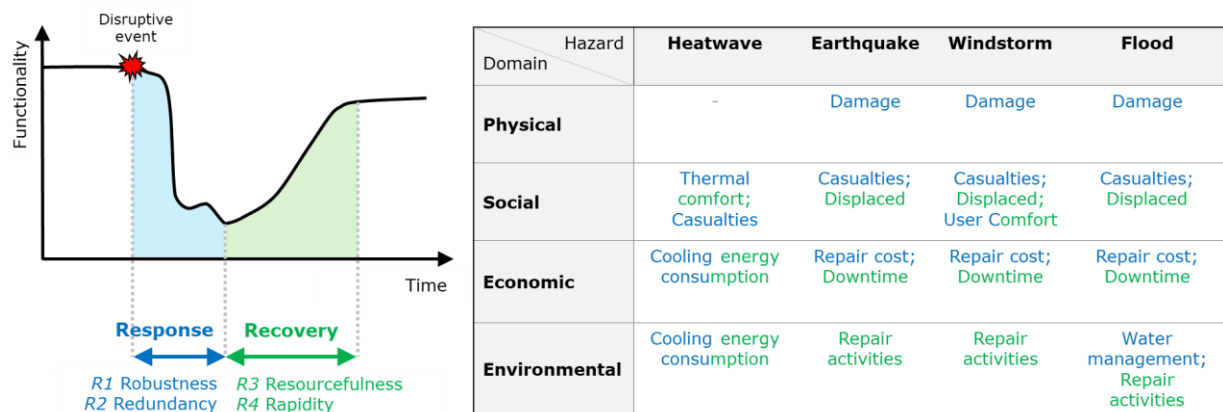


Figure 1. Consequences associated with each analyzed hazard, in both the response (blue) and recovery (green) phases

MULTICARE employs the latest developments in probabilistic risk assessment methods and frameworks, further enhancing them to facilitate a unified approach across various and diverse hazards. For instance, thermal fragility curves - representing the probability of reaching or exceeding, e.g., specific temperature thresholds based on thermal comfort levels - will be developed for European building archetypes. These curves provide a practical tool for integrating heat vulnerability with other physical vulnerabilities.

The losses quantified through these risk modeling approaches will yield robust decision variables, which will be integrated using a multi-criteria decision-making (MCDM) approach to quantify building resilience (see Deliverable D6.1). This process involves assigning weights to the variables based on the specific local context, stakeholder preferences or project constraints. These weighted factors are then combined to derive a unified resilience score and Resilience Readiness Level (RRL) of buildings. This score serves as a valuable metric for guiding the selection of optimal retrofit or design strategies, and supporting the prioritization of interventions for a building portfolio.

1.2.1 Objectives and method

This deliverable aims to compile the various sources of uncertainty involved in risk assessment and the probabilistic risk approaches used to quantify the expected losses for the hazards addressed in the MULTICARE project (**Figure 1**). Additionally, it outlines how this information is used to develop decision-support methods for determining multi-hazard resilience scores, as discussed in Deliverable D6.1. This multidisciplinary approach will enable better-informed decisions on resilience enhancement at scales ranging from buildings to building portfolios.

First, the deliverable provides a description of the sources of uncertainty involved in the vulnerability assessment, which include:

- **Hazard uncertainty**, encompassing record-to-record variability, referring to the differences in characteristics among individual hazard events, and hazard intensity variability, arising from the uncertainty in estimating the severity of the hazard itself.
- **Building uncertainty**, due to factors such as material properties, construction details, occupant behavior (e.g., heating and cooling preferences) and variability in consequence functions (e.g., repair costs, repair time). The latter are also influenced by the building's location, labor and material costs, the extent of damage, and local standards.
- **Modeling uncertainties**, related to the level of building definition, model quality and completeness, and the definition of thresholds to categorize building performance into damage states.

The deliverable then describes the building-level probabilistic risk assessment approaches developed or currently under development in the different disciplines, referencing existing literature and international guidelines while advancing these methods to address climate-induced hazards (e.g., heat). The deliverable concludes with a section detailing how the results from these probabilistic approaches are used to quantify multi-domain resilience. This approach builds upon the framework initially defined in Deliverable 6.1, with further developments presented here.

As part of this deliverable, open-access Python-based codes have been developed, and uploaded to the MULTICARE project's GitHub repository ([multicareConsortium](#)), to enable: (i) the evaluation of social, economic and environmental losses caused by extreme events with specific return periods; (ii) the estimation of a building's resilience score, which accounts for both its response and recovery capacity.

1.2.2 Relation to other activities

Table 2 illustrates the principal connections of this deliverable to other activities developed within the MULTICARE project, which should be taken into account alongside this document to gain a deeper understanding of its contents.

Table 2. Relation to other WPs

Work Package	Contribution
WP4 - Performance requirements, criteria and user's needs, and MULTICARE overall approach	This deliverable outlines the methodology for conducting risk assessment, integral to the overall project concept and for quantifying the selected loss-specific KPIs.
WP5 - Resilient-based framework and design tools for materials and building components	The uncertainty sources and risk methodologies outlined in this deliverable will be used to quantify the loss-specific performance indicators of building components.
WP7 - Spatial decision-support framework and system for multi hazard resilience analysis at urban level	This deliverable defines the risk assessment methods to be adapted and expanded for analyzing building portfolios, and integrated into the Spatial Decision Support Framework.
WP14 - Acerra – Preparation and Virtual demonstrator	This deliverable outlines the methodology for quantifying the consequences of extreme events, which will inform the selection of renovation or design scenarios for the case studies in the three European countries.
WP16 - Amsterdam – Preparation and Virtual demonstrator	
WP18 - Bucharest – Preparation and Virtual demonstrator	
WP21- Tecuci – Monitoring & Assessment	
WP23 - Impact assessment of the MULTICARE solutions	This deliverable provides the calculation methods for the indicators which describe the potential lifecycle impacts of the MULTICARE solutions.

2. Uncertainty in risk assessment

This chapter identifies the various sources of uncertainty involved in risk assessment. Addressing uncertainty is critical as it enables professionals to communicate effectively with decision makers, while avoiding perceived guarantees or liabilities associated with performance assessments.

Every factor influencing building performance carries uncertainty in predicting specific values. Uncertainty is commonly categorized as aleatory or epistemic:

- (i) **Aleatory uncertainty** refers to the natural randomness inherent in a process. For discrete variables, this is represented by the probability of each possible value. For continuous variables, it is characterized by a probability density function.
- (ii) **Epistemic uncertainty**, arises from limited data and knowledge about the process. For discrete random variables, this is modeled by assigning a scattering / confidence interval to each value, while for continuous random variables it is represented by probability density functions. Epistemic uncertainty can also affect parameters that are not random but have a single correct (but unknown) value.

Understanding and quantifying the various sources of uncertainty is essential for developing probabilistic models to guide effective risk and resilience assessment.

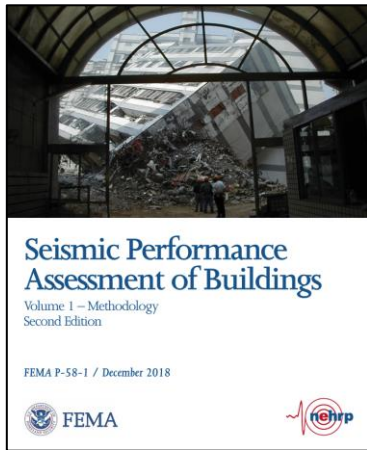
2.1 Hazard uncertainties

- **Record-to-record variability**

In structural risk assessments, particularly when a structure experiences a nonlinear response, each hazard record will produce different predictions of peak response quantities, leading to record-to-record variability. For example, in seismic risk analysis, variability in responses arises from the inherent differences in each ground motion record. Similarly, in the case of extreme weather events, variability emerges from the differing properties of the events.

Using a limited number of ground motion records or weather event data can result in significant inaccuracies when estimating record-to-record variability for response quantities. This may lead to underestimation or overestimation of dispersion values, compromising the reliability of the analysis. Additionally, demand correlation coefficients - representing the relationships between different response quantities - can also be inaccurately captured. To address this, a larger dataset (e.g., at least 30 ground motion records for seismic assessments) is typically recommended to better capture the variability and provide more reliable statistical estimates. However, many established methods, such as FEMA P-58 (2018), proceed under the assumption that record-to-record variability and demand correlation coefficients calculated using smaller sample sizes are sufficiently accurate. These methods mitigate potential inaccuracies by augmenting the analysis with additional sources of uncertainty.

When simplified analysis methods are used for performance assessments, it is important to integrate record-to-record variability for key demand parameters. For example, in the case of earthquakes, dispersion values are provided for parameters such as drift ratio, floor acceleration and floor velocity. As outlined in the FEMA P-58 (2018), these β values are defined based on the structure's natural vibration period and its strength ratio. However, dispersion values have not yet been calibrated for the other hazards under consideration.



T_1 (sec)	$S = \frac{S_a(T_1)W}{V_{y1}}$	$\beta_{u,d}$	$\beta_{a,a}$	$\beta_{v,v}$
0.20	≤ 1.0	0.05	0.10	0.50
	2	0.35	0.10	0.51
	4	0.40	0.10	0.40
	6	0.45	0.10	0.37
	≥ 8	0.45	0.05	0.24
0.35	≤ 1.0	0.10	0.15	0.32
	2	0.35	0.15	0.38
	4	0.40	0.15	0.43
	6	0.45	0.15	0.38
	≥ 8	0.45	0.15	0.34
0.5	≤ 1.0	0.10	0.20	0.31
	2	0.35	0.20	0.35
	4	0.40	0.20	0.41
	6	0.45	0.20	0.36
	≥ 8	0.45	0.20	0.32
0.75	≤ 1.0	0.10	0.25	0.30
	2	0.35	0.25	0.33
	4	0.40	0.25	0.39
	6	0.45	0.25	0.35
	≥ 8	0.45	0.25	0.30

Figure 2. Extract from Table 5-6 of FEMA P-58 (2018): dispersions for record-to-record variability for use with simplified analysis (where S represents the building strength, assessed from its weight W , the 5% damped spectral acceleration at the building's fundamental period $S_a(T_1)$, and the estimated yield strength of the building in its first mode response V_{y1})

Although not as pronounced as in the case of earthquakes, record-to-record variability in wind hazards remains a significant source of uncertainty. This variability arises due to differences in wind characteristics, such as speed profiles, turbulence intensity, and directional changes, across recorded events. The nature of the wind (e.g., synoptic events, hurricanes, tornadoes) significantly influences these characteristics, leading to diverse pressure distributions and time histories that affect structural responses. Quantifying these variations remains challenging due to the complex mechanics of wind flows and their interactions with structures and terrain (Ciampoli et al., 2011). Furthermore, spatial heterogeneity in wind speeds, induced by turbulence and environmental factors such as terrain roughness and obstacles, adds another layer of complexity (Blocken 2014).

Despite advancements in time history analysis for modeling wind effects, its widespread application is limited by high computational demands and the need for validation through wind tunnel testing. Adapting nonlinear time history analyses originally developed for seismic engineering has also proven difficult, as wind loads are non-zero mean actions, unlike seismic forces (NIST 2023). The complexity increases further when accounting for the impact of airborne debris, obstacles, or concurrent rain effects, each adding layers of variability and interaction. Consequently, the quantification of uncertainties in wind hazards remains an open and evolving area of research. The presence of debris and the wind profile are typically modeled based on terrain roughness, with wind profiles often defined as a combination of mean wind speed and a random zero-mean fluctuating component. The energy and behavior of wind-borne debris are commonly represented using distinct missile environments, (HAZUS FEMA 6.1 Hurricane). Wind speed distributions for use in time history analyses can be derived through various methodologies, including computational fluid dynamics (CFD) simulations or by combining deterministic and stochastic components to account for turbulence and variability (NIST 2023).

In the case of energy and thermal comfort assessment, variables related to temperature (dry bulb temperature, dew point temperature), precipitation (relative humidity), wind (wind direction, wind speed) and solar radiation (horizontal infrared radiation, global horizontal radiation, direct normal radiation, diffuse horizontal radiation) are used as weather input for building simulation tools and any discrepancies on them can cause inaccuracies in the simulation outcome. Weather information is typically described by (i) historical data through TMY (Typical Meteorological Year) files and (ii) future weather data which are generated considering future weather projections. In the first case, TMY files account for inter-annual record variability, i.e. differences in year-to-year weather records, through condensing data from multiple sequential years into one characteristic weather file. In the second case, global climate models (GCMs) are used to describe future climate variability at a large spatial resolution (100-300 km) capturing the large-scale circulation patterns (Nik and Sasic Kalagasidis 2013). However, data from GCMs must undergo spatial and temporal downscaling to generate information that (i) reflects local climatic conditions and (ii) is provided in hourly resolution respectively. The latter is particularly relevant to energy and thermal comfort assessment tools which necessitate hourly weather data input.

According to Berardi and Jafarpur (2020), three main methods have been introduced to translate climate change data into downscaled weather information; (i) extrapolating statistical method, (ii) imposed offset method and (iii) stochastic modelling. Among these, imposed offset method, and particularly morphing, has been most widely used in literature studies. Morphing relies on historical data and performs three operations; (a) “shifting” (adding on existing data), (b) “stretching” (multiplying existing data) or (c) combination of two operations. Thus, it is largely dependent on existing data and historical weather patterns are assumed to be maintained in future periods (**Figure 1Figure 3**). In contrast, stochastic method generates probabilistic weather data by modeling the variability and uncertainty inherent in climate systems. Rather than directly adjusting historical data (like morphing method), it randomly samples from distributions based on observed climate statistics and projected trends.

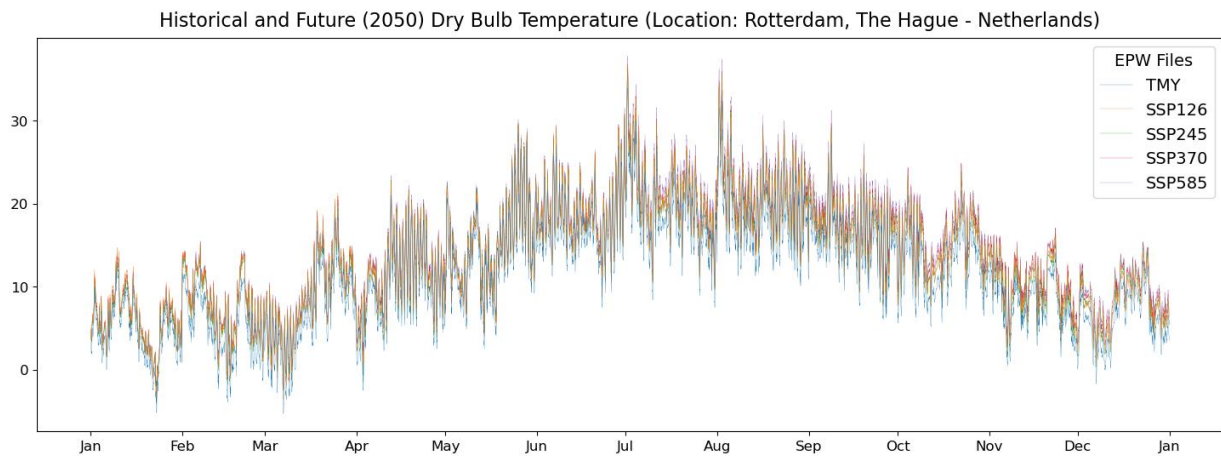


Figure 3. Annual dry bulb temperature values produced through morphing of TMY values according to different SSP scenarios for year 2050 (EC-Earth3 climate model). Morphing was performed using the future weather generator from Rodrigues et al. (2023)

- **Hazard intensity**

In time-based assessments, considering the likelihood of hazard events and their potential impacts over a specified time horizon (e.g., the building service life), hazard curves explicitly account for uncertainty in the intensity. However, in scenario-based assessments - focusing on the impacts of a specific hazard event - the variability in hazard intensity should be considered. This uncertainty directly impacts the demand used to evaluate building performance under different hazard scenarios. For instance, in seismic assessments, ground motion intensity is typically assumed to follow a lognormal distribution (**Figure 4**), characterized by a median value and a dispersion (β_{gm}), which accounts for the variability in ground motion characteristics such as amplitude and frequency content. The value of β_{gm} can be derived from earthquake histories statistically analyzed by fitting a lognormal distribution. FEMA P-58 (2018) also provides default values for β_{gm} based on different ground motion scenarios and building types. These values are derived from empirical data and analysis of ground motion characteristics, and they can be extrapolated or adjusted based on the specific characteristics of the building or region under consideration. In simplified analyses, ground motion dispersion is indirectly considered through the modeling uncertainty assumed in response calculations, which typically ranges from 0.25 to 0.50.

Beyond the immediate variability of individual events, broader uncertainties related to long-term climate variations and the increasing frequency and intensity of extreme events must also be considered. This includes the variability in long-term climate trends, such as rising temperatures and changing precipitation patterns, which affect flood and heat event intensities. Additionally, there is growing uncertainty regarding the occurrence, intensity, and duration of future extreme weather events, such as heatwaves, floods, and severe storms. Climate models project these changes, but they also introduce their own sources of variation that must be accounted for in scenario-based assessments, particularly when assessing the resilience of structures over long periods.

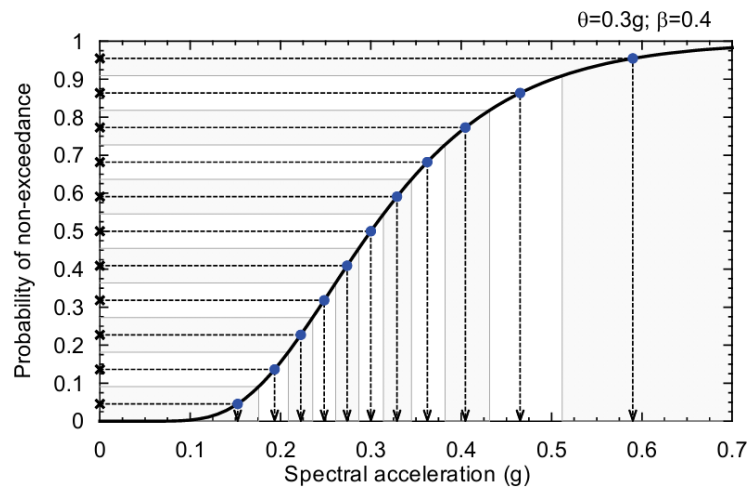


Figure 4. Example of cumulative probability distribution for a scenario earthquake (FEMA P-58 2018)

Intergovernmental Panel on Climate Change (IPCC) has developed distinct future pathway scenarios based on the expected rate of change in atmospheric concentrations and greenhouse gas emissions. In this regard, there are five different high-priority shared socio-economic pathway (SSP) scenarios corresponding to distinct socio-economic projections (Meinshausen et al., 2020). Particularly, SSP1-2.6 is related to a sustainable environmental condition, where the increase in temperature is maintained close to the goals of Paris Agreement. SSP2-4.5 is considered the “middle-of-the-road scenario”, while SSP3-7.0 and SSP5-8.5 correspond to medium-high and high reference scenarios respectively. Specifically, the latter one is defined as the scenario where fossil fuel use continues at a high rate in the coming years, but it has been mentioned as highly unlikely to become reality. Each scenario includes projections for 30-year climatological values centred around 2050, 2100 and 2150. Additional scenarios include the definition of dry and wet variants per SSP scenario based on the expected precipitation (Van Der Wiel et al., 2024). Lastly, climate sensitivity uncertainty refers to the climate response to the anthropogenic emissions described in each one of the climate scenarios. Particularly, it is related to the time that the warming levels are going to be achieved and, thus, it is model dependent. Van Der Wiel et al. (2024) suggests considering this type of uncertainty a posteriori, shifting the time horizon for reaching the warming level forwards or backwards according to the assumed climate sensitivity, e.g. high sensitivity would result in reaching the warming level earlier in time.

While evidence for a definitive trend in synoptic winds due to climate change remains inconclusive, climate change is anticipated to intensify hazards associated with non-synoptic wind events like hurricanes. Despite the substantial damages caused by windstorms in Europe in recent years, the scientific literature indicates a lack of consensus regarding their long-term trends in frequency and intensity under the influence of climate change (Spinoni et al., 2020). Moreover, uncertainties in wind intensity are highly dependent on the specific wind regime being analyzed. For instance, Petrini and Francioli (2022) have proposed a classification of uncertainties for buffeting and vortex-shedding regimes based on data from the NIST database.

When focusing on floods, these are among the most challenging natural events to predict, primarily due to the substantial variability in the environmental conditions that can trigger such events and the complexity of accurately forecasting their timing and magnitude at specific locations. Forecasting flood durations, depths and velocity is a challenging process influenced by numerous factors. Among the factors contributing to these uncertainties are meteorological, hydrological, topographical, as well as data limitations. There is also a significant impact of topography and geomorphology on flood behavior. In order to estimate flood extent and depth accurately, digital elevation models (DEMs) must be accurate, as errors can misrepresent the terrain (Diaconu et al., 2021). Changes in land use and cover, such as urbanization and deforestation, may alter runoff patterns and result in increased flooding. The geometry of channels, including their dimensions and roughness, can also influence flow velocity and depth estimates. Several other factors contribute to flood uncertainty, including rainfall intensity and distribution. Forecasting models may not be able to capture precise movements, intensities, and durations of storm systems due to variable rainfall patterns, especially during extreme events. Soil moisture conditions are another critical factor, as the initial saturation level determines the capacity for infiltration and influences runoff predictions (Costache & Zaharia, 2017). Furthermore, interactions between surface water and groundwater, which are often poorly understood, can complicate flood modeling.

Data limitations present another significant challenge. Inaccurate historical records of past flood events can lead to flawed model calibration and validation (Costache et al., 2019). Measurement devices, such as rain gauges and streamflow sensors, may introduce errors or contain gaps in the data. Temporal discontinuities in rainfall or discharge records can result in incomplete representations of flood dynamics, further complicating predictions. Modeling assumptions and limitations add another layer of complexity. Simplifications of physical processes, such as turbulence or wave interactions, can result in approximate outcomes, and scenario-based assumptions, like peak rainfall intensity or dam break conditions, heavily influence the accuracy of predictions. External factors, including tidal influences in coastal areas or variations in snowmelt and glacial inputs, further complicate flood estimation. The assessment of flood magnitude relies heavily on historical measurements from specific river sections, with the recognition that the most severe event may yet occur. Designations of recurrence intervals, such as 10-, 100-, or 1,000-year events, remain relevant until surpassed by future extremes, highlighting the inherent uncertainty in flood hazard evaluations.

2.2 Building uncertainties

Besides hazard-related variability, building uncertainties also play a significant role. In energy and thermal comfort, several studies utilize probabilistic assessment frameworks to assess their impact on the final simulation outcome (Bianchi et al., 2022). The uncertainties can be caused by (i) inherent data variability, such as measurement errors, (ii) exterior influences, such as moisture, temperature and ageing, and (iii) lack of knowledge about the current building condition, such as unavailability of records related to existing retrofit interventions. The latter is mostly relevant for simulations at building stock level, where the input is frequently based on data from archetype clustering and might not represent

accurately the realistic conditions. A detailed description of the different categories is provided below.

Similarly, earthquakes, windstorm and flooding are influenced by uncertainties related to building characteristics. Some of these uncertainties are aleatoric, such as the mechanical properties of materials, while others stem from the level of knowledge about the building, including factors like construction age, material types, and the details of both structural and non-structural elements, including building contents.

- **Material properties**

Heat losses through the building envelope play a large role in the total building energy demand. Therefore, the thermal properties of the envelope components constitute an indispensable input of the energy simulations and, specifically, the most influential material properties are:

- ✓ **thermal conductivity** (W/mK), which indicates the material capacity for heat transfer
- ✓ **density** (kg/m³), referring to the ratio of mass per volume unit
- ✓ **specific heat capacity** (J/kgK), referring to the quantity of heat needed per mass unit to increase the material temperature by one-degree Celsius
- ✓ **relative roughness** of material surface
- ✓ **thermal and solar absorptivity**, referring to the ability of material to absorb wavelength and solar radiation

Tian, et al. (2018) provides a review of literature studies that describe the inherent variability and measurement errors in the parameters through probabilistic distributions. The variability is usually expressed with normal and gaussian distributions which are defined based on experimental data or literature studies (**Table 3**).

Table 3. Uncertainty studies on inherent variability and measurement errors in material properties

Variable	Distribution	Reference
Thermal conductivity, density, specific heat capacity of diverse building materials & non-massive layers	Normal	Macdonald (2002) Hopfe and Hensen (2011) Rodríguez et al. (2013)
Thermal conductivity, specific heat capacity of timber, concrete and insulation materials	Normal	IEA (1991) Prada et al. (2018)

Besides inherent variability, literature studies investigate the impact of external factors in the deterioration of material thermal performance. Among them, moisture saturation, temperature and ageing are mentioned to be the most influential parameters. In this regard, Domínguez-Muñoz et al. (2010) describes the insulation thermal conductivity as a function of density, moisture content, temperature and age and proposes different function coefficients based on the insulation material. Ageing has received particular attention and several studies evaluate the impact of ageing in the building energy demand. Although the non-stationarity of deterioration because of ageing has been acknowledged

and models such as Gamma processes would be more adequate to use (De Wilde et al., 2011), the lack of data to create detailed models leads frequently to the adoption of fixed yearly degradation rates (**Table 9**). Ferreira et al. (2023) refers to Markovian models for the expression of mechanical degradation of envelope components but, to the knowledge of authors, there is no existing study on the expression of material thermal conductivity as a Markovian model.

Table 4. Studies applying fixed yearly rates to express the deterioration of thermal performance because of ageing

Variable	Approach	Reference
Thermal conductivity	Standard yearly degradation rate	De Wilde et al. (2011)
	Best and worst-case scenarios for yearly degradation effect	Waddicor et al. (2016)
Window decay due to silicon, sealant and paint layer degradation as well as gas leakage	Yearly energy performance decay rate	Litti et al. (2018)
Gas leakage and coating degradation in insulated glass units, deterioration of thermal conductivity in insulation materials	Definition of distinct degradation scenarios for yearly degradation rate	Taki and Zakharanka (2023)

When focusing on the other hazards, the material properties also represent an important uncertainty source. For wind hazard, this become much more important in the case of high-rise buildings, where wind actions represent a strong design constraint. The most influential material properties are:

- ✓ **strength** (kPa), which indicates the material capacity to sustain stress before yielding / breaking
- ✓ **stiffness** (kPa), referring to the effective mechanical stiffness of the material
- ✓ **damping ratio** (%), referring to the ability of the structural system of given material to dampen vibrations

Material properties can be determined through observed data or material testing. The dispersion and uncertainties associated with these properties are strongly linked to the quality control of the materials themselves. Some materials inherently have greater uncertainty in their mechanical properties, such as concrete, compared to steel. Typically, material properties are modeled using normal or lognormal distributions. Additionally, the aging of components, particularly concrete, must be considered to account for the effects of aging over time.

- **Construction details**

The thermal properties of each material layer are jointly used to define the thermal resistance (R) or transmittance (U) of the whole envelope component. In this regard, Ohlsson et al. (2022) estimates the model error and uncertainty of window U value considering the uncertainties of input variables of all parts of the window assembly. Similarly to deterioration in material thermal properties, studies examine the effect of

degradation in the total R and U values through yearly degradation rates (**Table 5**). Liu et al. (2022) further extends the framework accounting for reduction in the effectively insulated area because of damage and falls of material. This is described as a time-variant Weibull variable and uncertainty around the variable is sampled from a normal distribution (**Figure 5**).

Table 5. Studies examining the effect of ageing on component thermal resistance / transmittance

Variable	Approach	Reference
Thermal Resistance (R)	Long-Term Thermal Resistance as an expression of aging on the R-value	Tariku et al. (2023)
Thermal Transmittance (U)	Thermal transmittance expressed as a uniform distribution where minimum is the design value and maximum corresponds to a standard increase of 30% because of humidity effect	Carpino et al. (2022)
	Effect of age in component U value through a yearly ageing factor. To account for stochasticity in the ageing factor (due to non-stationary rate of material degradation or maintenance), the expected U value at every timestep is modelled as a normal distribution whose standard deviation becomes larger along with the ageing of building	Liu et al. (2022)
	Evaluation of ageing effect on gas leakage in insulated glass units, effect of gas leakage scenarios in component U value	Asphaug et al. (2016)

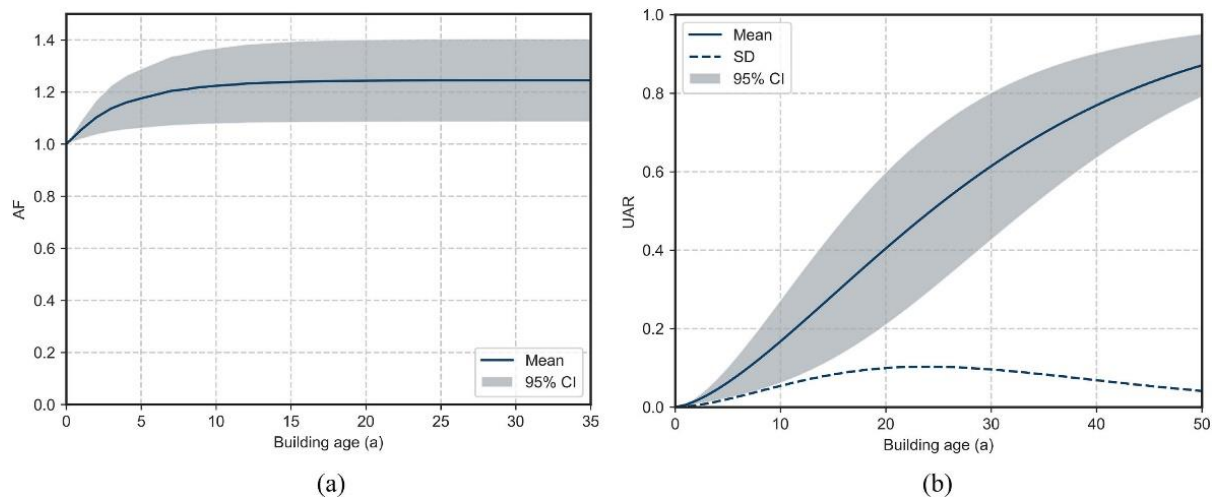


Figure 5. Stochasticity in age factor (AF) and uninsulated area ratio (UAR) of the building envelope as described in (Liu et al., 2022)

Given the increasing interest in urban building energy simulations, studies expand uncertainty analysis at a larger scale. Prativiera et al. (2022) suggests broadening the assumptions regarding variability of R/U values when simulations at building stock level are performed to account for additional uncertainties that may be underlying. In this

regard, triangular distributions are introduced to describe the U values of windows and opaque structures. The minimum and maximum values of the distributions correspond to extreme variability scenarios. Alternatively, Van Hove et al. (2023) proposes a two-step sampling where the first step refers to the variation among the building stock and, at every timestep, the mean and standard deviation of the normal distributions describing each parameter are sampled from uniform distributions. The second one includes sampling from the normal distributions to extract the building-level information (**Figure 6**).

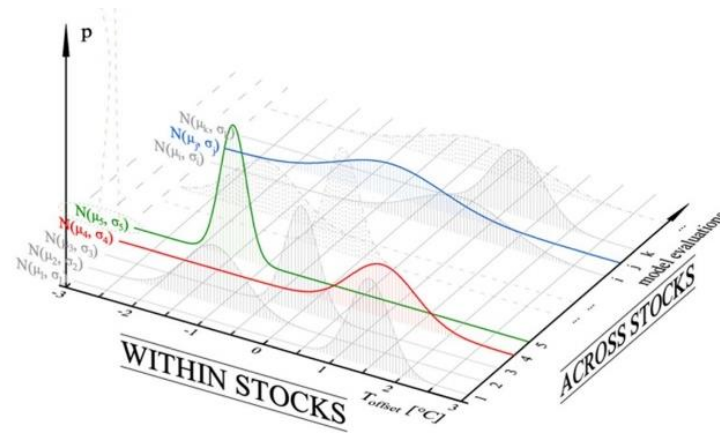


Figure 6. Sampling across and within building stocks (Van Hove et al., 2023)

Finally, another important parameter of the envelope construction is infiltration which refers to the uncontrolled flow of air in the building interior through gaps and cracks of the envelope surface. The variability in the parameter is usually expressed with normal distributions (

Table 6).

Table 6. Variability in infiltration rate

Variable	Distribution	Reference
Infiltration	Normal	Hopfe and Hensen (2011) Macdonald (2002) Rodríguez et al. (2013)
	Scenarios of effect in infiltration due to sealant degradation and appearance of cracks in the envelope	Taki and Zakharanka (2023)

In the context of wind hazards, uncertainties related to construction details often arise from variations in component-level solutions that lead to differing overall performance. Examples of such details include how HVAC components are bolted to rooftops or uncertainties in the number and type of connections used to secure built-up roofs to the structure. These uncertainties are typically incorporated into fragility functions at the component or building level, alongside limit state threshold uncertainties. Usually, such fragility curves are modeled by means of Normal, Lognormal, or Weibull distributions

(**Table 7**). Additionally, uncertainties in construction details can stem from the aerodynamic properties of the structure. These uncertainties often dominate the dynamic behavior of tall structures but can also significantly influence the distribution of wind pressures around the building envelope.

Table 7. Key uncertainties associated with construction detailing

Variable	Distribution	Reference
Roof component resistance	Normal	Gurley et al. (2005)
	LogNormal	Datin et al. (2011) Prevatt et al. (2008)
Openings resistance	Normal	Peng (2013)
Building envelope failure due to pressure	Weibull	Liang and Memari (2012)
Building envelope failure due to debris impact	LogNormal	Zhang et al. (2013) McDonald (1990)

Construction details also play a critical role in determining the impact of earthquakes and floods. The quality and design of connection details—such as beam-to-column joints, base connections, and anchorage systems—directly influence the structure's ability to withstand seismic forces. Poorly detailed connections can lead to premature failures, which compromise the overall structural integrity. Features such as the presence of openings, the design of walls, and the specifications of window fixtures can significantly affect the floodwater's entry and the resultant interior water height. Additionally, the spatial distribution of these elements around the building's perimeter can influence which sections are more prone to flooding. Another factor introducing uncertainty in flood scenarios is the height at which components and contents are placed relative to the ground. Floodwater presence at a specific level often leads to a binary outcome for contents: they are either damaged or remain intact. To model this uncertainty, Nofal et al. (2020) proposed using a truncated normal distribution, which accounts for the maximum and minimum possible positions of a given content.

- **Building Occupant**

Besides the uncertainties in the building parameters which are the most common aspect to be considered in building uncertainty analysis (Fenell et al., 2019), there are other parameters that can introduce variability in the energy demand, such as occupant behavior and natural ventilation schedules. Particularly, Guo et al. (2025) mentions that fluctuations in occupant behavior can result in larger uncertainty in heat demand than building parameters.

Occupant behavior uncertainty encompasses how the building is operated, including daily occupancy patterns and how occupants use lighting, air conditioning systems and equipment. The key parameters for assessing and improving building overheating and thermal resilience related to occupancy behavior are summarized **Table 8**. The occupancy profile (i.e., elderly occupancy) and occupancy status (e.g., daytime absence) have significant impacts on overheating exposure. Stochastic occupancy time-series data can

be generated using high-temporal resolution residential building occupancy models for specific occupancy profiles (Buttitta et al., 2020). A simpler approach is available through the FEMA P58 Occupancy population model (FEMA P-58-1, Appendix E), which provides distributions of people and their temporal variations throughout the day and year for different building types.

Table 8. Uncertainties in occupant behavior

Variable	Distribution	Reference
Residential building stochastic occupancy model	Stochastic	Buttitta et al. (2020)
External shading control schedule	Binary	-
Night cooling control schedule	Binary	-
Window operation set point	Discrete	Silva et al. (2013)
Cooling set point	Normal	ASHRAE Standard 55 (2020)
Heating set point	Normal	ASHRAE Standard 55 (2020)

- **Consequence functions**

An extensive database of consequence functions related to repair costs of components is available in the FEMA P-58 guidelines. Although the data primarily pertains to earthquake-induced damage, the consequences of damage from other sources can often be assumed to be similar to those considered for earthquakes. The uncertainties related to consequences are closely tied to the type of Key Performance Indicator (KPI) that needs to be computed. FEMA P-58 (2018) defines consequence curves for both downtime and repair costs (**Figure 7**).

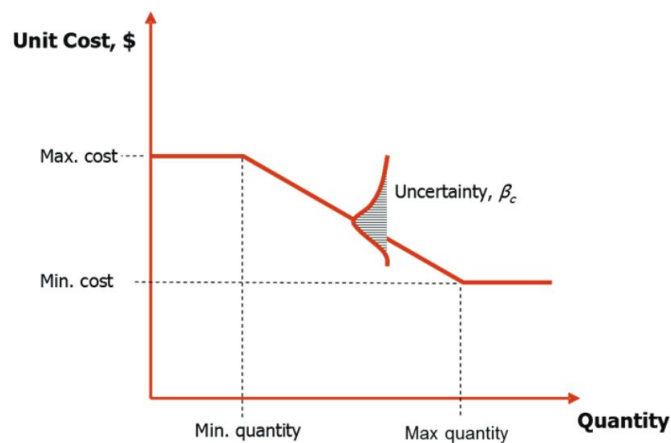


Figure 7. Uncertainty related to consequence functions based on component quantity (FEMA P-58 2018)

These consequence function uncertainties can be applied to individual components as well as to the damage states of entire structures (Aljawhari et al., 2023; Aljawhari et al., 2024; Hazus FEMA 6.1 Earthquake). Component uncertainties are generally influenced by both the type of component and its volume. For components categorized as "long lead time," additional uncertainties arise from market availability, as these components may need to be manufactured on demand, as outlined in the REDi guidelines. Furthermore, downtime

is influenced by additional uncertainties related to "impeding factors" (HAZUS FEMA 6.1 Earthquake, REDi). These factors refer to delays in repairs that are not directly caused by component damage but result from external influences. Impeding factors can significantly impact the time between the event and the initiation of repairs. These consequences apply to multiple hazards involving a repair phase and are typically categorized into inspection, design, financing, contractor mobilization, and permitting. The uncertainties associated with these aspects are modeled as lognormal functions, with values reported in the REDi earthquake guidelines.

2.3 Modelling uncertainties

- **Building definition**

This modeling uncertainty addresses the possibility that the actual geometrical properties of building elements may differ from those assumed or documented in the analysis. This uncertainty arises from the inherent variability in how buildings are constructed, as well as the limitations of available data. The dispersion associated with this uncertainty (β_c) is assigned based on the confidence and quality of the building's definition. According to the FEMA P-58 (2018), dispersion values can be assumed equal to 0.10, 0.25 and 0.40 in case of superior, average or limited quality assurance, respectively.

For existing buildings, this dispersion is influenced by the quality and completeness of available documentation, such as architectural and structural drawings that describe the 'as-built' condition. The dispersion is further impacted by the extent of field investigations conducted to verify the actual construction. The greater the level of detail and verification through fieldwork, the smaller the dispersion value, reflecting higher confidence in the building's real geometrical properties. For new buildings, the dispersion is based on assumptions regarding the quality control processes in place during construction and how accurately the built structure will match the original design. If the design is expected to be executed with high precision and quality control, the dispersion value will be smaller. If there are uncertainties regarding construction practices, the dispersion value will be larger to account for potential discrepancies between the design and actual construction.

This type of uncertainty is particularly affecting building portfolio analysis. For example, since there are no detailed models for every building in the city, energy simulations largely rely on geometric data extracted from public GIS databases and archetype classification. Prataiviera et al. (2022) utilizes uniform distributions to describe uncertainties in the area of external walls and internal partitions as well as net volume because of discrepancies in LiDAR detection and geometry modelling. Van Hove et al. (2023) assesses the impact of uncertainties in building orientation on the total energy performance. Sampling from normal distribution is performed to define the mean values across the building stock, while sampling from log-normal distribution is conducted to define the standard deviation that describes the uncertainty within the building stock. Guo et al. (2025) states that the optimal set of explanatory variables comprises postal code, building type, construction year, protected volume and roof area, among which postal code is mentioned as the most influential. In this study, the correlation of different building parameters is also examined

creating multivariate Gaussian distributions from the Gaussian distributions of the uncorrelated parameters.

Similar to energy simulations, large-scale assessments for wind, seismic and flood hazards often lack detailed building-specific information. Consequently, much of the required data must be inferred from available sources, introducing an additional layer of uncertainty. This uncertainty can be mitigated by conducting more thorough assessments or collecting more comprehensive data on the building stock. Such data collection can be achieved through in situ inspections, as discussed above, or remote sensing technologies.

The characteristics of a building can generally be classified into three categories:

- ✓ **structural**, referring to the structural elements of the building, such as the size, location, and material properties of load-bearing components
- ✓ **non-structural**, including the building envelope and all components that are part of the building but do not contribute to load-bearing functions
- ✓ **contents**, encompassing the objects and equipment housed within the building

For earthquakes, extreme wind and flooding, uncertainties related to building non-structural components can be modelled using the FEMA P-58 (2018) distributions (**Figure 8**). These distributions are based on an extensive survey of building types conducted across the United States and are categorized by specific building use classes. These uncertainties are typically not addressed directly but are instead incorporated into the modelling of archetypes. Archetypes are representative models designed to capture the characteristics and behaviors of a broader building class.

Component Type	Unit of Measurement	10 th Percentile Quantity	50 th Percentile Quantity	90 th Percentile Quantity
Gross area	SF	5,000	34,000	582,200
Volume	CF per 1 gsf	7.440	10.460	14.500
Cladding				
Gross wall area	SF per 1 gsf	0.320	0.770	1.300
Windows or glazing area	100 SF per 1 gsf	6.0E-04	1.5E-03	3.0E-03
Roof area - total	SF per 1 gsf	0.090	0.320	1.000
Interior partition length	100 LF per 1 gsf	7.0E-04	1.2E-03	1.6E-03
Ceramic tile floors	SF per 1 gsf	0.108	0.212	0.340
Ceramic tile walls	100 LF per 1 gsf	1.9E-04	3.8E-04	6.1E-04
Ceilings				
Ceiling - lay in tile percentage	%		0%	
Ceiling - gypsum board percentage	%		95%	
Ceiling - exposed percentage	%		5%	
Ceiling - other (high end) percentage	%		0%	

Figure 8. Normative Quantities for Multi-Unit Residential Occupancies – Extract from Table F-5 of FEMA P-58 (2018)

- **Quality and completeness of the model**

This modeling uncertainty recognizes that analytical models – e.g., used to describe the nonlinear behavior of components under load - may not always accurately represent the real-world performance of those components, even when construction details are well-known. This is due to the complexities in how materials and components behave under loading and extreme conditions, which may not be fully captured by the model. Values of this uncertainty (β_q) are therefore assigned based on the completeness and fidelity of the mathematical model used to simulate the behavior of the structure. For instance, a model that comprehensively accounts for material degradation, fatigue and inelastic behavior is expected to have lower dispersion than one with a more simplistic or incomplete representation of these mechanisms. FEMA P-58 (2018) provides default values for this dispersion based on the quality of the analytical model used in the simulation (**Table 9**).

Table 9. Dispersion values for quality of the analytical model

Quality assurance	Dispersion β_q
Superior quality – model accurately capturing structural and energy behaviors, including deterioration, failure modes, and performance, while incorporating all relevant components and validated by experiments	0.10
Average quality – model capturing displacement, deformation and energy performance with reasonable accuracy, including most structural and nonstructural components, and validated through judgment and tests	0.25
Limited quality – model based on idealized cyclic envelope curves, without direct incorporation of strength, stiffness deterioration, or failure modes. It includes only relevant structural and non-structural components.	0.40

- **Thresholds values**

This uncertainty stems from the difficulty in precisely defining when a building reaches certain damage conditions (e.g., for earthquake, wind, flood) or comfort thresholds (e.g. for heatwave, wind) due to the complexity of interactions between materials, occupants and environmental conditions. The thresholds for identifying different levels of damage (e.g., slight, moderate, severe) can vary depending on the model and assumptions used. In some cases, damage thresholds are based on expert judgment, which introduces uncertainty due to differences in interpretation and experience. Comfort thresholds (e.g., for standard effective temperature) are often based on guidelines or standards, but individual perceptions of comfort can vary widely. Factors like personal preferences, health conditions and acclimatization are difficult to model and introduce uncertainty. Comfort thresholds can also change depending on environmental conditions (e.g., the combination of heat and humidity), which are difficult to predict especially in extreme or fluctuating scenarios.

2.4 Summary

This chapter has provided a comprehensive review of the multifaceted sources of uncertainty in risk modeling for buildings under various hazard scenarios. The summary, illustrated in **Figure 9**, highlights the diverse aspects of uncertainty. References throughout the chapter outline methodologies for representing these uncertainties within probabilistic building simulations.

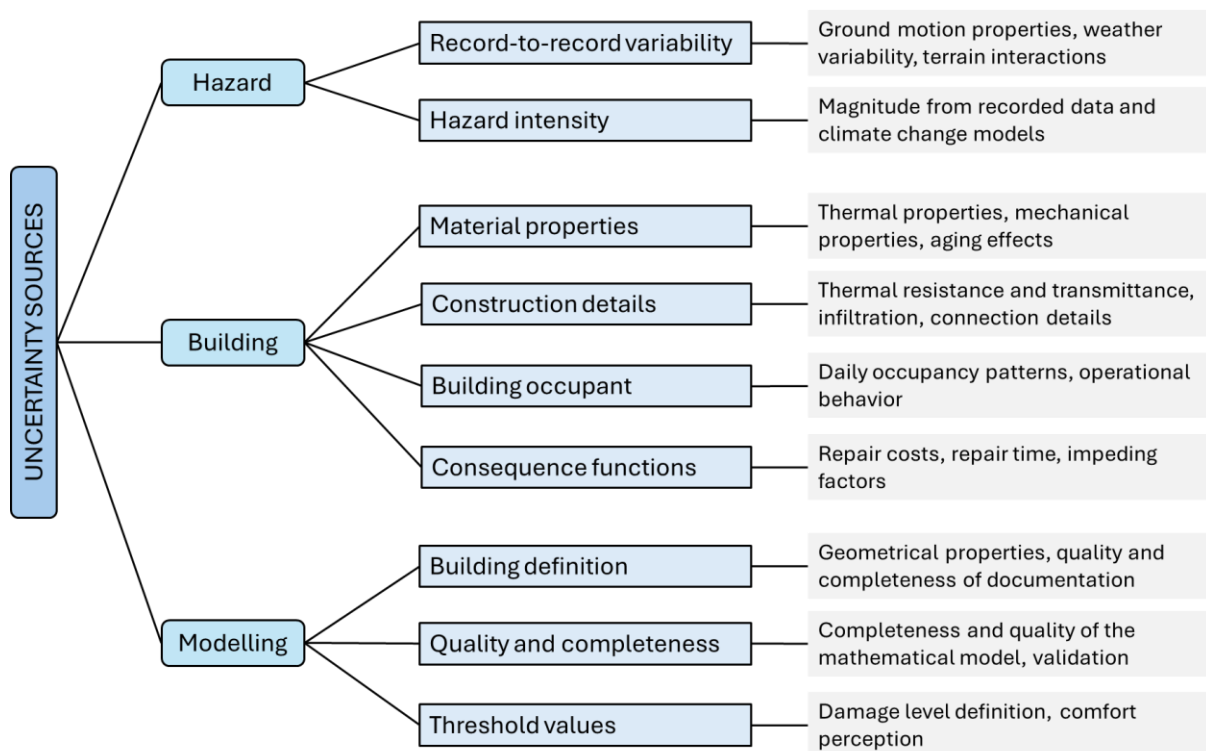


Figure 9. Uncertainty sources in risk modelling

As part of the MULTICARE project, these uncertainties will be incorporated into various studies, including risk assessments (as detailed in the next chapter), sensitivity analyses to understand the impact of specific parameters on resilience quantification, and surrogate modeling for performance evaluation. Building upon this initial classification of uncertainties, the next step involves defining these uncertainties for the building archetypes identified at the MULTICARE demonstration sites. This will enable the development of a comprehensive catalogue that can serve as a valuable resource for similar studies in the future.

3. Risk assessment of buildings

This deliverable outlines the risk modeling methodologies employed to quantify the impacts of extreme events studied in the MULTICARE project. A consistent probabilistic approach is applied to each hazard, where risk is defined as the likelihood of experiencing a specific consequence - such as repair costs, downtime, injuries, fatalities, population displacement or carbon emissions. Risk is conceptualized as a combination of three key factors, described below in alignment with the definitions provided by the Arup Universal Taxonomy (Arup, 2024):

- (i) **Hazard**, representing the probabilistic likelihood and associated intensity of a hazard impacting the building over a specified future time period. For hyperlocal hazards, such as flooding, the spatial resolution must be sufficiently high to accurately reflect the hazard's severity at the building's footprint.
- (ii) **Vulnerability**, defining the probability that building components sustain a particular level of damage given the intensity of the hazard. For occupants, impacts may arise directly from the hazard (e.g., heat exposure) or indirectly (e.g., falling debris caused by earthquakes).
- (iii) **Exposure**, encompasses the location, type, value and capacity of structural, architectural and mechanical components, as well as the building's functional uses. Additionally, it accounts for the number and vulnerability of the building's occupants.

When assessing risk for a specific hazard, the uncertainties outlined in the previous section are taken into account. Typically, a Monte Carlo simulation is employed to quantify these uncertainties. This method uses probabilistic sampling techniques to account for the randomness and variability inherent in each variable of the risk assessment.

3.1. Seismic risk

Seismic hazard is typically expressed in terms of the frequency distribution of a ground motion parameter, such as peak ground acceleration, over a specified time interval. It reflects the potential intensity of an earthquake event that could cause physical impacts to buildings or occupants (Arup, 2024). The hazard intensity is measured at the building location and can be deterministic (e.g., for a defined magnitude) or, preferably, probabilistic. In the probabilistic approach, each intensity level is associated with a likelihood or probability of occurrence. This is often conveyed as return periods or the probability of exceedance within a given year or over a specified time horizon. Seismic hazard data is generally derived from historical seismic observations and extrapolated to estimate the likelihood of rare future events.

To define vulnerability, i.e. the susceptibility of a building to damage or impairment due to a hazard event, mathematical functions are used to relate hazard or demand parameters to the extent and severity of damage to buildings, their components, and contents. In earthquake engineering, the Performance-Based Earthquake Engineering (PBEE)

methodology (e.g., Cornell et al., 2002; Krawinkler and Miranda, 2004) provides a systematic approach for vulnerability assessment (Figure 10).

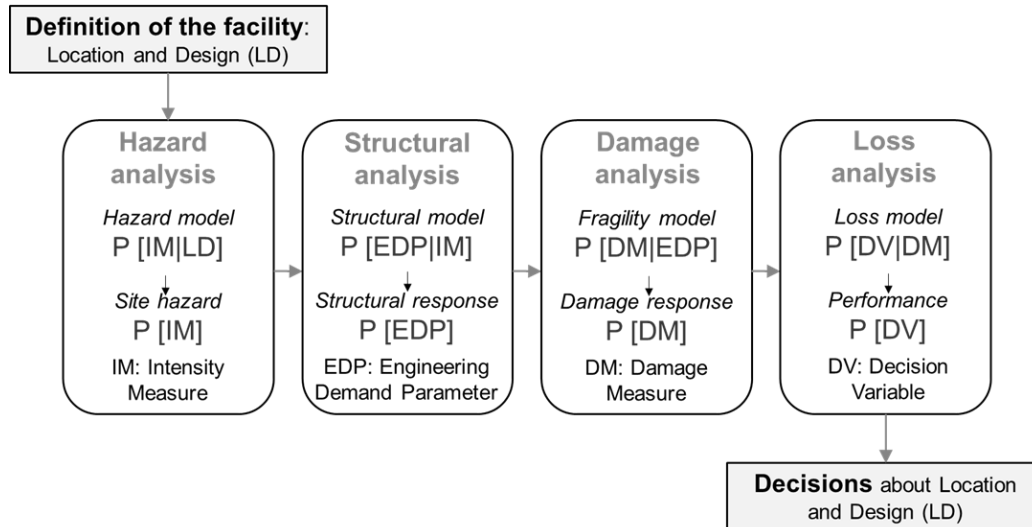


Figure 10. PEER framework for loss modelling

The methodology provides a robust framework for understanding and mitigating seismic risks, aligning engineering outcomes with stakeholder priorities. The process begins by defining the seismic hazard, typically characterized by parameters such as ground motion intensity. The building's structural response is then evaluated in terms of engineering demand parameters, such as floor accelerations or inter-story drift ratios. The system's response is linked to the damage experienced by each building component. The damage is typically defined in terms of fragility curves, which are statistical distributions used to indicate the probability that a component, element or system will be damaged as a function of a predictive demand parameter. Fragility functions typically take the form of lognormal cumulative distribution functions, having a median value, θ , and logarithmic standard deviation, or dispersion, β :

$$F_i(D) = \Phi \left(\frac{\ln \left(\frac{D}{\theta_i} \right)}{\beta_i} \right)$$

where $F_i(D)$ is the conditional probability that the component will be damaged to damage state “i” (or more severe damage state) as a function of a demand parameter, D ; Φ denotes the standard normal (Gaussian) cumulative distribution function; θ_i denotes the median value of the probability distribution; and β_i denotes the logarithmic standard deviation (FEMA P-58 2018). Finally, damage measures are translated into decision variables - repair costs, repair time or casualty estimates - that guide decision-making processes for seismic risk mitigation. The methodology can be expressed in terms of a triple integral based on the total probability theorem, which provides the loss function $\nu(DV)$ considering the inherent uncertainties in all phases of the problem. This also provides a consistent format for sharing and integrating data and models developed by researchers in the various disciplines (Moehle and Deierlein, 2003).

$$v(DV) = \iiint G\langle DV|DM \rangle | dG\langle DM|EDP \rangle | dG\langle EDP|IM \rangle d\lambda(IM)$$

Moreover, to estimate indirect economic losses, a critical parameter for post-disaster functional recovery, the PEER methodology's outputs on repair time are integrated with probabilistic functions outlined in the REDi Guidelines. These functions account for delays associated with scheduling inspections, mobilizing workers and materials, and securing financing for repairs, providing a comprehensive framework for assessing recovery timelines.

3.2. Wind risk

For wind scenarios, the hazard involves determining the wind velocity at 10 meters above the ground. In Europe, these values can be assessed using the Eurocode 1 (2002) and the national annexes. This assessment may need to be adjusted to account for the effects of exposure and the terrain roughness surrounding the building, as these factors significantly influence the local wind environment. Additionally, it is essential to model the expected missile environment, as the number and energy of debris impacting the structure depend not only on wind speed but also on the characteristics of the building's surroundings. Another critical aspect to evaluate is the concurrence of rain, given the cascading effects it can have on building contents and finishes. The presence of rain during wind events is strongly influenced by the storm's originating mechanism, whether it arises from synoptic systems, hurricanes, or funnel clouds.

Each building component is then assigned a capacity, which can be determined using engineering demand parameters, such as surface pressure or impact energy, or intensity measures, such as the 3-second gust wind speed (as referenced in Hazus v6.1 for Hurricanes). The sampling of actions on these components allows for the estimation of the probability of damage to building envelope elements, including windows, walls and roofs. It is important to recognize that wind damage can propagate, leading to cascading effects where the failure of one component increases the vulnerability of others. To model these cascading events, fault tree models can be used effectively. These models account for damage to internal components as well as the interaction of multiple hazard mechanisms, providing a comprehensive approach to understanding and modeling damage progression (Merhi et al., 2025), as shown in **Figure 11**.

After a damage scenario has been modeled by sampling both actions and capacities, loss quantification can be conducted using a component-based approach as outlined in FEMA P-58 for earthquakes. Additionally, downtime can also be modeled by employing the REDi framework, which provides a structured methodology to incorporate factors such as impeding factors, utility disruption and repair sequence into its assessment.

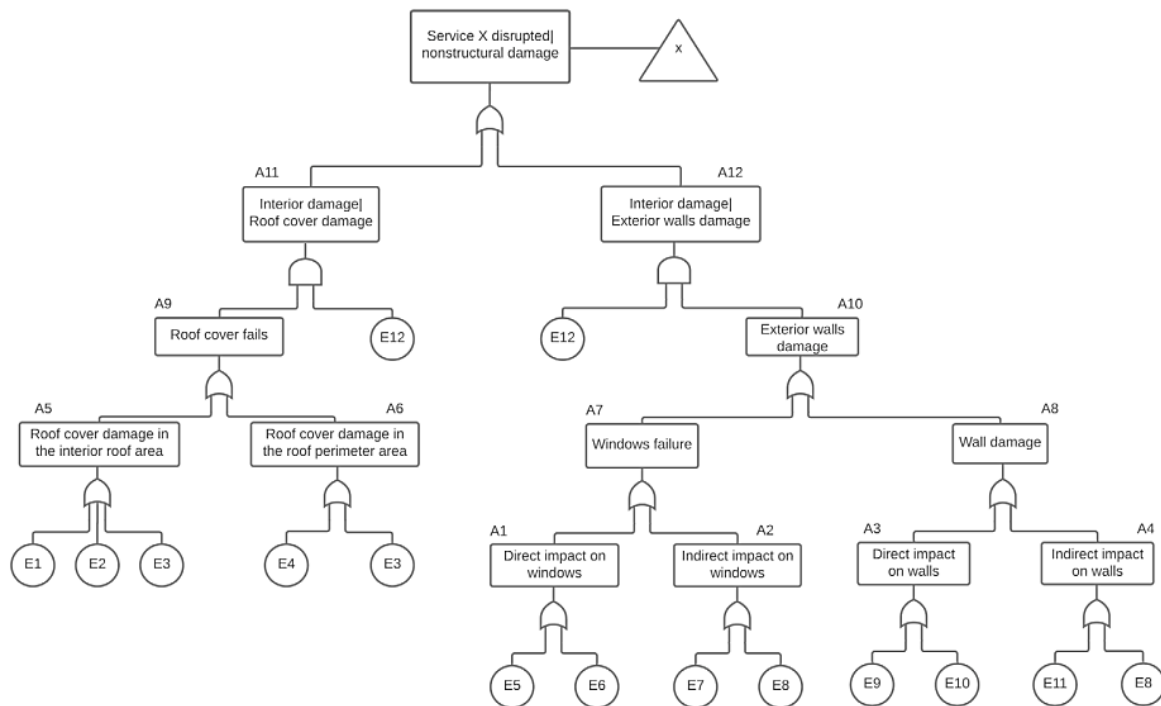


Figure 11. Fault tree for a service disruption given the occurrence of nonstructural damage (Merhi et al., 2025)

3.3. Flood risk

Flood hazard scenarios are typically much more sensitive to the specific location of a building compared to hazards such as wind, heat or earthquakes. Typically, hydrological models are used to estimate intensity measures such as flood depth, velocity and duration. The quality of hydrological models improve significantly with a reduction in the size of the individual cells used to compute flood depth, where "cells" refer to the individual grid units that divide the region being analyzed into smaller sections. Flood hazard evaluations can be performed using digital terrain models or by incorporating building footprints. In many cases, the size of the cells for which flood depth is resolved is smaller than the footprint of the building itself. This mismatch necessitates an additional step to correlate the spatial distribution of water depth around the building with the resolution used in the analysis that feeds into the hazard curve. Flood hazard data can be obtained by running custom simulation models using software tools (e.g. HEC-RAS). Alternatively, hazard data can be sourced from trusted hazard providers (e.g. Fathom, SaferPlaces), offering precomputed hazard assessments for specific locations with different cell sizes (e.g. 30 sqm).

Fragility functions for each building component are determined based on the expected elevation of the component within the building. These fragility curves capture the uncertainty associated with the flood elevation that would result in the failure or write-off of the component or the contents. To compute the vulnerability curve, that relates a damage ratio to the intensity measure (e.g., flood depth), fragility curves are integrated for various hazard intensities (Nofal et al. 2020, **Figure 12**).

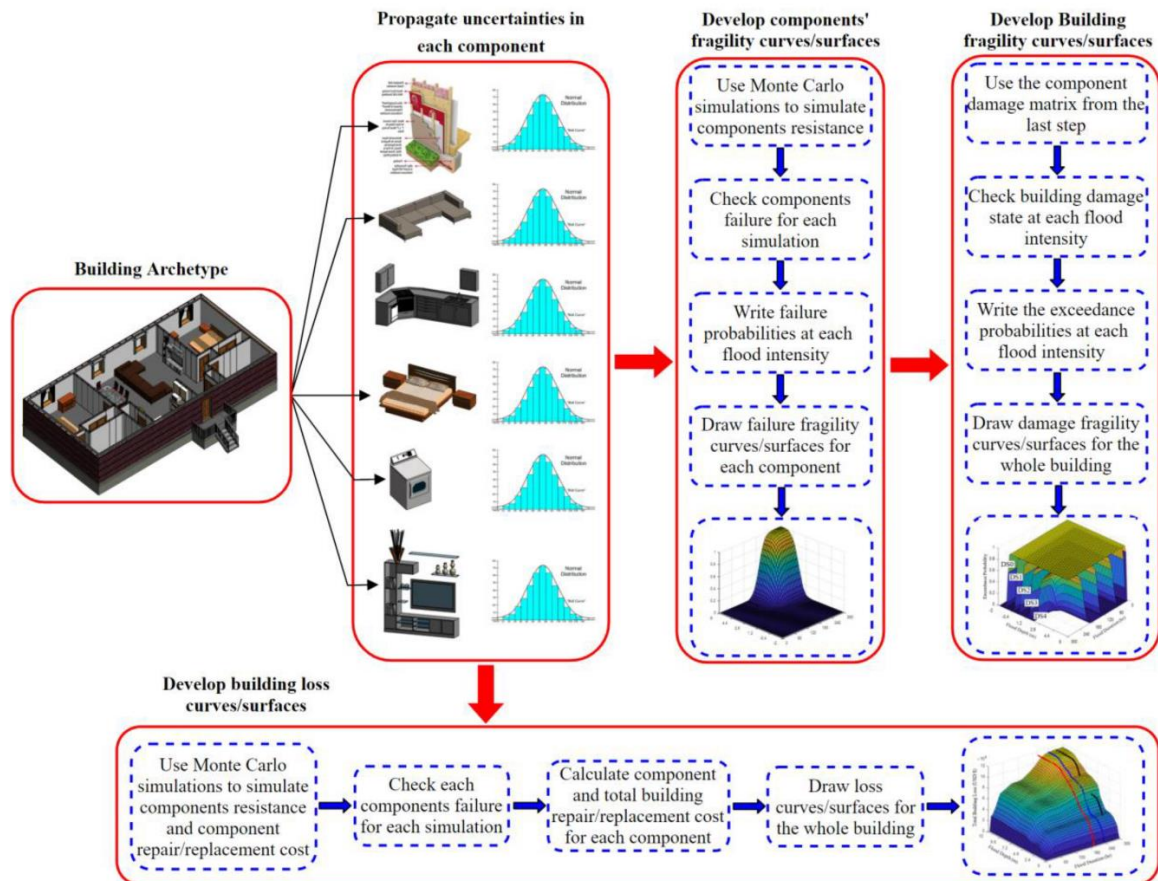


Figure 12. Loss modelling framework proposed by Nofal et al. (2020)

In flood assessments, the internal flood depth is typically chosen as the engineering demand parameter. This parameter can be modeled by correlating the flood depth relative to the first-floor elevation of the building, providing a clear measure of the potential impact on internal components and contents (Paulik et al., 2022). This approach ensures that the analysis accurately reflects the vulnerability of individual components to varying flood conditions. Flood loss quantification can be then performed using a component-based approach similar to the one outlined in FEMA P-58 for earthquakes, while also integrating downtime calculations as described in the *REDi for flood* framework. This framework provides functions that identify delays before initiating repair actions, including the duration of floodwaters, restoration mobilization and cleanup, engineer mobilization and permitting, financing of repairs and contractor mobilization.

3.4. Heat risk

For heat-related shocks, severity indicates how much the outdoor temperature deviates from typical conditions, while duration measures how long the shock lasts. Sengupta et al. (2024) classified and quantified degree of shock (doS) to compare different heatwaves and their impact on thermal resilience. Their research identified 6 representative extreme heatwaves in Ghent, Belgium projected for 2001-2100, categorizing them as most severe,

most intense, or longest. They then analyzed the key design parameters affecting thermal resilience for these different degrees of shock. As for the other hazard types, both historical data and future projections can be used to derive hazard curves considering a specific intensity measure, such as extreme temperature or heat index.

To define the heat vulnerability, the application of fragility curves remains relatively unexplored, with only a few recent efforts proposing analytical formulations for thermal fragility curves (Szagri et al. 2022, Kim et al. 2024). Kim et al. (2024) introduced a methodology for deriving thermal fragility curves by adapting existing fragility analysis methods. **Figure 13** summarizes the derivation process. The study selected outdoor dry bulb temperature (DBT) and daily maximum DBT as intensity measures (IMs), while the indoor standard effective temperature (SET) was used as the engineering demand parameter (EDP). Two analytical methods—multiple stripe analysis and cloud analysis—were applied to these IM-EDP pairs across various temperature thresholds. Dynamic thermal modeling and simulation were conducted over a one-year period using synthetic weather files generated to account for future heatwaves. The results demonstrated how the selection of IM indicators, EDP thresholds, and analytical fragility derivation methods influence the fragility curves and their interpretation. As part of the MULTICARE project, future research will aim to identify more precise IM-EDP pairs to accurately represent the relationship between heatwave events and indoor thermal conditions, including the impact of thermal history. Additionally, fragility analysis should address uncertainties related to natural ventilation operation and building envelope properties, as this study considered only heatwave event variability in the derivation of fragility curves.

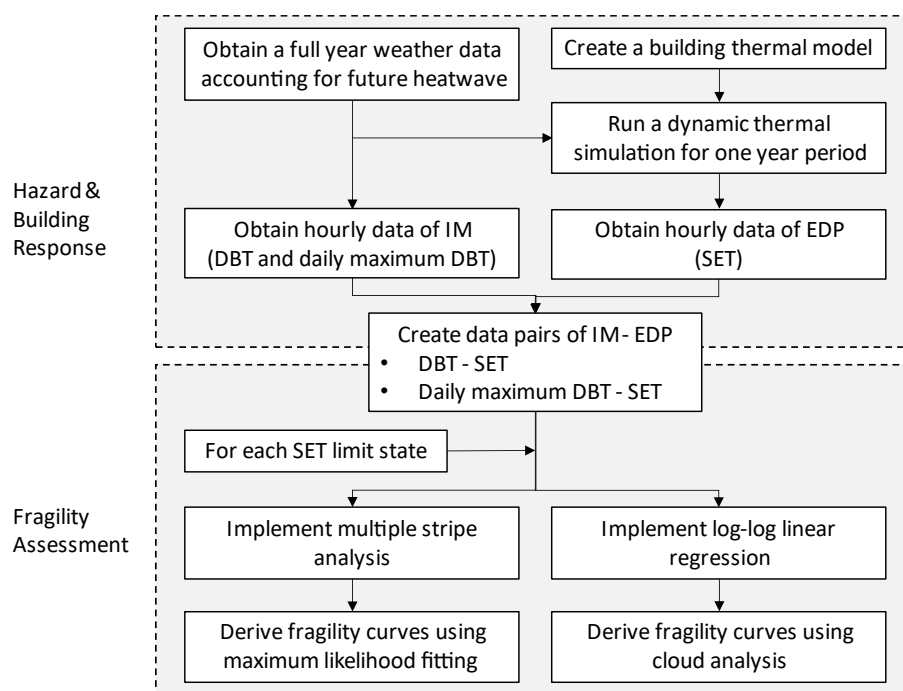


Figure 13. Thermal fragility curves derivation process (Kim et al, 2024)

Finally, to define vulnerability models, heatwave-related losses can be computed in terms of cooling load or electricity consumption required to mitigate health impacts, as well as direct measures of heat exposure consequences, such as discomfort levels or mortality rates. To quantify the latter, relationships between mean daily temperature and the relative risk of death should be considered. For example, studies such as those by Gasparrini et al. (2015) have demonstrated temporal variations in heat-mortality associations based on daily time series, revealing U- or J-shaped patterns. These relationships enable to assess the social impact caused by heatwaves in a specific location.

4. Resilience quantification

MULTICARE adopts the risk assessment methods outlined in the previous section, which are based on the latest frameworks developed across various disciplines. These methods will be further enhanced (e.g., for heat risk analysis) to quantify the expected losses for buildings, as identified in **Table 10**.

Table 10. Resilience indicators derived from loss modelling

Hazard	Phase	Domain	Description
Earthquake	Response	Social	Number of deaths
		Economic	Repair Cost [cost/m ²]
	Recovery	Economic	Downtime [months]
		Environmental	Carbon emissions [kg CO ₂ e/m ²]
Wind	Response	Social	Number of deaths
		Economic	Repair Cost [cost/m ²]
	Recovery	Economic	Downtime [months]
		Environmental	Carbon emissions [kg CO ₂ e/m ²]
Flood	Response	Social	Number of deaths
		Economic	Repair Cost [cost/m ²]
	Recovery	Economic	Downtime [months]
		Environmental	Carbon emissions [kg CO ₂ e/m ²]
Heat	Response	Social	Number of deaths
		Environmental / Economic	Cooling energy consumption [kWh/m ²]
	Recovery	Environmental / Economic	Cooling energy consumption [kWh/m ²]

These variables are part of the resilience indicators that define both the response and recovery capacity of buildings under extreme events. They are integral to the decision-making approach outlined in Deliverable D6.1 to derive Resilience Readiness Levels for buildings. Specifically, a multi-criteria index is derived from the normalized values of these resilience indicators, where normalization is based on building properties (e.g., number of occupants, replacement cost, replacement time, and carbon footprint) or reference / threshold values from existing codes and guidelines, as discussed in Deliverable D6.1. Multi-hazard resilience scores can be thus calculated for buildings, enabling direct comparisons

between the resilience levels of different as-built structures or design/retrofit options in a multi-hazard context. An example of applying this method (**Figure 14**) is provided in **Appendix A**, which focuses on two demo sites (Amsterdam, Acerra), with the calculation of resilience scores also available as Python code on the MULTICARE GitHub repository ([multicareConsortium](https://github.com/multicareConsortium)).

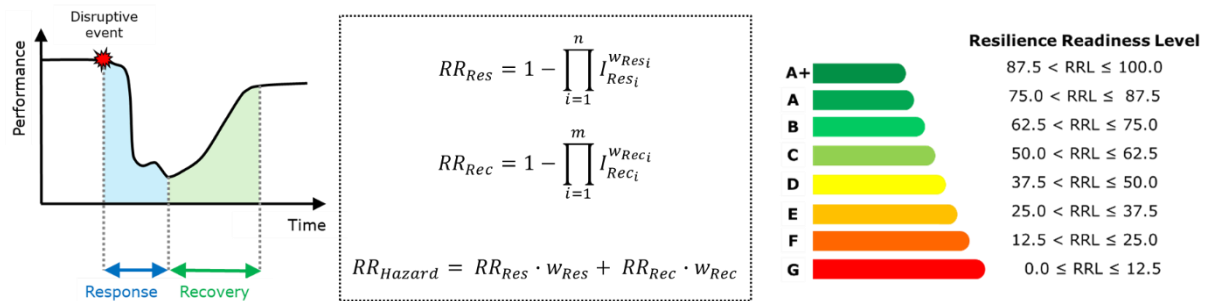


Figure 14. Resilience Readiness (RR) calculation method, where “I” indicates the different resilience indicators identified in Deliverable D6.1 and “w” the selected weighted factors

In addition to calculating multi-domain resilience scores, these variables can also be used to derive resilience curves for specific hazards. For example, in seismic resilience (**Figure 15**), the level of building damage and repair costs can be used to evaluate the building’s robustness to seismic hazards and defining the functionality drop for a specific intensity-based event. The recovery phase for an individual building following disruption is closely linked to the downtime and environmental losses required to achieve a defined recovery state, such as re-occupancy, restoration of pre-earthquake functionality and full recovery. Similarly, resilience curves can be derived for the other hazards.

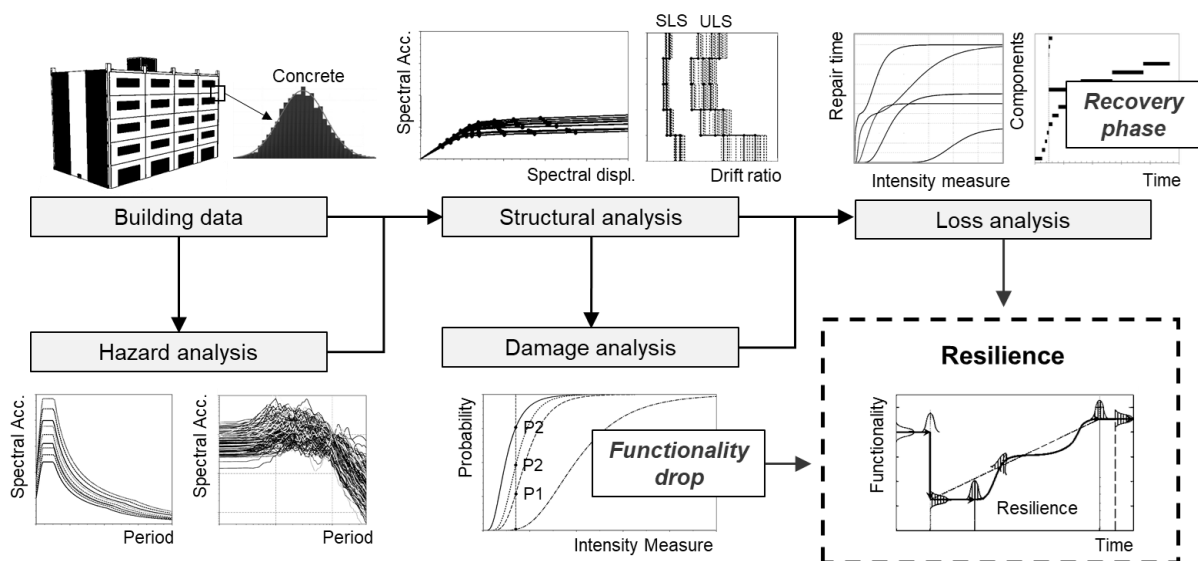


Figure 15. Derivation of seismic resilience curves

Moreover, the loss-based variables (repair cost, downtime, casualties and carbon emissions) can be assessed using either time-based methods (annualized values) or intensity / scenario-based assessments, which focus on the impact of specific hazard levels or event scenarios (probable maximum loss). The choice between these methods depends on the preferences of the decision-makers, with time-based methods supporting long-term risk management strategies and event-based assessments helping insurers determine risk-based premiums. Both types of assessments will be incorporated into the framework of the MULTICARE project.

5. Conclusions

This deliverable has detailed the loss modeling approaches employed in the MULTICARE project to assess social, economic and environmental consequences arising from climate-induced extreme events (heat, flood, wind) and natural disasters (earthquakes). A key focus has been the consideration of uncertainties - aleatoric and epistemic - across various dimensions, including hazard characteristics, building attributes, occupancy, consequences and threshold values. These uncertainties are incorporated into building-level risk modelling methods tailored to different hazards, integrating probabilistic modelling and numerical simulations to estimate expected annualized or probable maximum impacts on buildings. The deliverable has introduced and referenced these methods, emphasizing the well-established approaches for earthquakes, newly developed methods for floods and wind, and ongoing advancements for heat.

The resulting loss estimates serve as inputs to the resilience quantification framework outlined in Deliverable D6.1, enabling a multi-domain (social, economic, environmental, and physical) holistic assessment of building resilience. These quantified losses form the basis for a multi-criteria decision-making process, culminating in a unified resilience score for buildings. This comprehensive approach advances the ability to evaluate and enhance building resilience under multi-hazard conditions.

As part of WP6, the loss modeling approaches and resilience score calculation will be made available as Python scripts on the MULTICARE GitHub repository, promoting transparency and accessibility for stakeholders. Additionally, this resilience score will serve as a key component of a decision-support digital tool for early-stage design or retrofit decision-making. The tool will facilitate resilience quantification for buildings at the project demo sites, as preliminarily outlined in the appendix of this deliverable.

6. References

- Aljawhari, K., Gentile, R., & Galasso, C. (2023). Simulation-based consequence models of seismic direct loss and repair time for archetype reinforced concrete frames. In *Soil Dynamics and Earthquake Engineering* (Vol. 172, p. 107979). Elsevier BV.
- Aljawhari, K., Gentile, R., & Galasso, C. (2024). Earthquake-induced environmental impacts for residential Italian buildings: Consequence models and risk assessment. In *Journal of Building Engineering* (Vol. 84, p. 108149). Elsevier BV.
- Arup (2024) A Universal Taxonomy for Natural Hazard and Climate Risk and Resilience Assessments.
- ASHRAE. (2020). Standard 55 – Thermal Environmental Conditions for Human Occupancy.
- Asphaug, S., Jelle, B., Gullbrekken, L., & Uvsløkk, S. (2016). Accelerated ageing and durability of double-glazed sealed insulating window panes and impact on heating demand in buildings. *Energy and Buildings*, 116, 395-402.
- Buttitta, G., Finn, D.P. (2020) A high-temporal resolution residential building occupancy model to generate high-temporal resolution heating load profiles of occupancy-integrated archetypes, *Energy and Buildings*, 206, 109577.
- Berardi, U., & Jafarpur, P. (2020). Assessing the impact of climate change on building heating and cooling energy demand in Canada. *Renewable and Sustainable Energy Reviews*, 121, 109681.
- Bianchi, S., Ciurlanti, J., Overend, M., & Pampanin, S. (2022). A probabilistic-based framework for the integrated assessment of seismic and energy economic losses of buildings. *Engineering Structures*, 269, 114852.
- Blocken, B. (2014) 50 years of Computational Wind Engineering: Past, present and future, *Journal of Wind Engineering and Industrial Aerodynamics*, 129, 69-102.
- Calleja Rodríguez, G., Carrillo Andrés, A., Domínguez Muñoz, F., Cejudo López, J., & Zhang, Y. (2013). Uncertainties and sensitivity analysis in building energy simulation using macroparameters. *Energy and Buildings*, 79-87.
- Carpino, C., Bruno, R., Carpino, V., & Arcuri, N. (2022). Improve decision-making process and reduce risks in the energy retrofit of existing buildings through uncertainty and sensitivity analysis. *Energy for Sustainable Development*, 68, 289–307.
- Cornell, C.A., Jalayer, F., Hamburger, R.O., & Foutch, D.A. (2002) Probabilistic basis for 2000 SAC Federal Emergency Management Agency steel moment frame guidelines. *ASCE Journal of Structural Engineering*, 128, 4, 526-533.
- Costache, R., & Zaharia, L. (2017). Flash-flood potential assessment and mapping by integrating the weights-of-evidence and frequency ratio statistical methods in GIS environment—case study: Bâsca Chiojdului River catchment (Romania). *Journal of Earth System Science*, 126(4), 59.
- Costache, R., Hong, H., & Wang, Y. (2019). Identification of torrential valleys using GIS and a novel hybrid integration of artificial intelligence, machine learning and bivariate statistics. *Catena*, 183, 104179.
- Datin, P. L., Prevatt, D. O., & Pang, W. (2011). Wind-Uplift Capacity of Residential Wood Roof-Sheathing Panels Retrofitted with Insulating Foam Adhesive. In *Journal of Architectural Engineering* (Vol. 17, Issue 4, pp. 144–154). American Society of Civil Engineers (ASCE).

- De Wilde, P., Tian, W., & Augenbroe, G. (2011). Longitudinal prediction of the operational energy use of buildings. *Building and Environment*, 46, 1670-1680.
- Diaconu, D. C., Costache, R., & Popa, M. C. (2021). An overview of flood risk analysis methods. *Water*, 13(4), 474.
- Domínguez-Muñoz, F., Anderson, B., Cejudo-López, J., & Carrillo-Andrés, A. (2010). Uncertainty in the thermal conductivity of insulation materials. *Energy and Buildings*, 42, 2159-2168.
- European Committee for Standardization (2005). "EN 1991-1-4 (2005) (English): Eurocode 1: Actions on structures - Part 1-4: General actions - Wind actions". European Committee for Standardization, Brussels, Belgium.
- FEMA (2008). Flood Damage - Resistant Materials Requirements for Buildings Located in Special Flood Hazard Areas. Technical Bulletin, 50. National Flood Insurance Program.
- FEMA (2018) Seismic Performance Assessment of Buildings, Volume 1 – Methodology. Washington D.C.: Federal Emergency Management Agency.
- FEMA (2022). HAZUS Hurricanes Technical Manual: Hazus 5.1. Department of Homeland Security, Washington D.C.: Federal Emergency Management Agency.
- FEMA (2024). "Hazus Earthquake Model Technical Manual – v6.1". Department of homeland security, Washington, DC, USA.
- Ferreira, C., Silva, A., De Brito, J., & Flores-Colen, I. (2023). Maintainability of Building Envelope Elements: Optimizing Predictive Condition-Based Maintenance Decisions. Cham: Springer International Publishing.
- Gasparrini, A., Guo, Y., Hashizume, M. et al. (2015). Temporal Variation in Heat–Mortality Associations: A Multicountry Study. *Environmental Health Perspectives*, 123(11), 1200-1207.
- Guo, R., Shamsi, M., Sharifi, M., & Saelens, D. (2025). Exploring uncertainty in district heat demand through a probabilistic building characterization approach. *Applied Energy*, 124411.
- Gurley, K., Pinelli, J., Subramanian, C., Cope, A., Zhang, L., Murphree, J., Artiles, A., Misra, P., Culati, S., and Simiu, E. (2005). Florida public hurricane loss projection model engineering team final report. International Hurricane Research Center, Florida International University.
- Hopfe, C., & Hensen, J. (2011). Uncertainty analysis in building performance simulation for design support. *Energy and Buildings*, 43, 2798-2805.
- IEA. (1991). IEA Annex XIV—Condensation and Energy—Catalogue of Material Properties. Birmingham: UK: International Energy Agency.
- Kim, K., Bianchi, S., Konstantinou, T., Overend, M., Ciurlanti, J., & Luna-Navarro, A. (2025). Thermal Resilience to Extreme Heat: Preliminary Study on Thermal Fragility Curves. In: Berardi, U. (eds) *Multiphysics and Multiscale Building Physics*. IABP 2024. Lecture Notes in Civil Engineering, vol 553. Springer, Singapore.
- Krawinkler, H., & Miranda, E. (2004) Performance-based earthquake engineering. *Earthquake Engineering: from engineering seismology to performance-based engineering*. Bertero VV (eds), CRC Press: Boca Raton.
- Liang, J., & Memari, A. M. (2012). Performance of a Panelized Brick Veneer Wall System under Lateral Loads. In *Open Journal of Civil Engineering* (Vol. 02, Issue 03, pp. 132–146). Scientific Research Publishing, Inc.

- Litti, G., Audenaert, A., & Lavagna, M. (2018). Life cycle operating energy saving from windows retrofitting in heritage buildings accounting for technical performance decay. *Journal of Building Engineering*, 17, 135-153.
- Liu, Z., Zhou, X., Tian, W., Liu, X., & Yan, D. (2022). Impacts of uncertainty in building envelope thermal transmittance on heating/cooling demand in the urban context. *Energy and Buildings*, 273, 112363.
- Macdonald, I. (2002). *Quantifying the Effects of Uncertainty in Building Simulation*. University of Strathclyde.
- McDonald, J. R. (1990). Impact resistance of common building materials to tornado missiles. In *Journal of Wind Engineering and Industrial Aerodynamics* (Vol. 36, pp. 717-724). Elsevier BV.
- Meinshausen, M., Nicholls, Z., Lewis, J., Gidden, M., Vogel, E., Freund, M., . . . Wang, R. (2020). The shared socio-economic pathway (SSP) greenhouse gas concentrations and their extensions to 2500. *Geoscientific Model Development*, 13, 3571-3605.
- Merhi, A., Andow, B., Cruzado, H., Letchford, C., & Lombardo, F. (2025). A framework for post-windstorm functional recovery of non-residential buildings applied to hospitals. In *Reliability Engineering & System Safety* (Vol. 253, p. 110508). Elsevier BV.
- MIT (Ministry of Transportation and Infrastructures, I. I. (2018). *NTC2018 - Normative Tecniche delle Costruzioni 2018*. Rome: Gazzetta Ufficiale.
- National Institute of Standards and Technology. "Extreme Wind Speeds: Data Sets".
- Nelson, M. B. (2022). *REDi™ Rating System: Resilience-based Design Initiative for the Next Generation of Buildings, Extreme Windstorms*.
- Nik, V., & Sasic Kalagasidis, A. (2013). Impact study of the climate change on the energy performance of the building stock in Stockholm considering four climate uncertainties. *Building and Environment*, 60, 291-304.
- Nofal, O. M., van de Lindt, J. W., & Do, T. Q. (2020). Multi-variate and single-variable flood fragility and loss approaches for buildings. In *Reliability Engineering & System Safety* (Vol. 202, p. 106971). Elsevier BV.
- Ohlsson, K., Nair, G., & Olofsson, T. (2022). Uncertainty in model prediction of energy savings in building retrofits: Case of thermal transmittance of windows. *Renewable and Sustainable Energy Reviews*, 168, 112748.
- Peng, J., Shan, X. G., Gao, Y., Kesete, Y., Davidson, R. A., Nozick, L. K., & Kruse, J. (2014). Modeling the integrated roles of insurance and retrofit in managing natural disaster risk: a multi-stakeholder perspective. In *Natural Hazards* (Vol. 74, Issue 2, pp. 1043-1068). Springer Science and Business Media LLC.
- Petrini, F., & Francioli, M. (2022) Next generation PBWE: Extension of the SAC-FEMA method to high-rise buildings under wind hazards. *Structural Safety* 99: 102255.
- Prada, A., Pernigotto, G., Baggio, P., & Gasparella, A. (2018). Uncertainty propagation of material properties in energy simulation of existing residential buildings: The role of buildings features. *Building Simulation*, 11, 449-464.
- Prataviera, E., Vivian, J., Lombardo, G., & Zarrella, A. (2022). Evaluation of the impact of input uncertainty on urban building energy simulations using uncertainty and sensitivity analysis. *Applied Energy*, 311, 118691.
- Prevatt, D. O., Schiff, S. D., Stamm, J. S., & Kulkarni, A. S. (2008). Wind Uplift Behavior of Mechanically Attached Single-Ply Roofing Systems: The Need for Correction Factors in Standardized Tests. In *Journal of Structural Engineering* (Vol. 134, Issue 3, pp. 489-498). American Society of Civil Engineers (ASCE).

- Rodrigues, E., Fernandes, M., & Carvalho, D. (2023). Future weather generator for building performance research: An open-source morphing tool and an application. *Building and Environment*, 233, 110104.
- Szagri, D., & Szalay, Z. Theoretical fragility curves – A novel approach to assess heat vulnerability of residential buildings. *Sustainable Cities and Society*, 83, 103969.
- Spinoni, J., Barbosa, P., Bucchignani, E., et al. (2020). Future Global Meteorological Drought Hot Spots: A Study Based on CORDEX Data. In *Journal of Climate* (Vol. 33, Issue 9, pp. 3635–3661). American Meteorological Society.
- Taki, A., & Zakharanka, A. (2023). The Impact of Degradation on a Building's Energy Performance in Hot-Humid Climates. *Sustainability*, 1145.
- Tariku, F., Shang, Y., & Molleti, S. (2023). Thermal performance of flat roof insulation materials: A review of temperature, moisture and aging effects. *Journal of Building Engineering*, 76, 107142.
- Tian, W., Heo, Y., De Wilde, et al. (2018). A review of uncertainty analysis in building energy assessment. *Renewable and Sustainable Energy Reviews*, 93, 285-301.
- Van Der Wiel, K., Beersma, J., Van Den Brink, et al. (2024). KNMI'23 Climate Scenarios for the Netherlands: Storyline Scenarios of Regional Climate Change. *Earth's Future*, 12, e2023EF003983.
- Van Hove, M., Delghust, M., & Laverge, J. (2023). Uncertainty and sensitivity analysis of building-stock energy models: sampling procedure, stock size and Sobol' convergence. *Journal of Building Performance Simulation*, 16, 749-771.
- Waddicor, D., Fuentes, E., Sisó, L., Salom, J., Favre, B., Jiménez, C., & Azar, M. (2016). Climate change and building ageing impact on building energy performance and mitigation measures application: A case study in Turin, northern Italy. *Building and Environment*, 13-25.
- Willford, I. A. (2013). REDi™ Rating System: Resilience-based Earthquake Design Initiative for the Next Generation of Buildings. Retrieved from
- Zhang, X., Hao, H., & Ma, G. (2013). Laboratory test and numerical simulation of laminated glass window vulnerability to debris impact. In *International Journal of Impact Engineering* (Vol. 55, pp. 49–62). Elsevier BV.

Appendix A - Preliminary results

Amsterdam case study

Heatwaves are critical for the city of Amsterdam (Netherlands) and this hazard was considered for the resilience score calculation of a mixed-use block in the inner city (Figure A1), consisting of buildings with diverse properties. Specifically, six different building archetypes were identified, characterized by residential or mixed use with commercial spaces on the first floor, with or without cooling systems (Table A1).

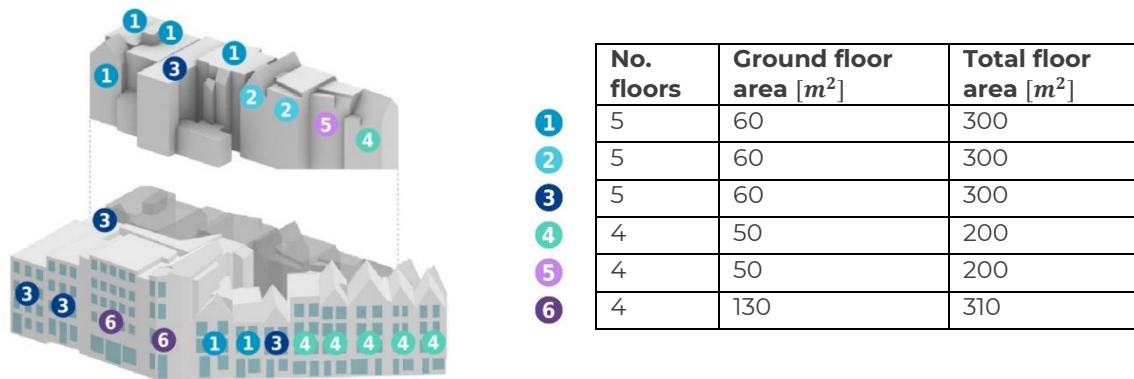


Figure A1. Urban block analyzed in Amsterdam, with index numbers indicating the building archetype. The compactness ratio is calculated as the ratio of all exposed envelope surfaces to the total building volume.

Dynamic energy simulations of the archetypes were performed in Rhinoceros 3D using the parametric interface of Grasshopper, a graphical algorithm editor that enables energy simulations with EnergyPlus. Building layouts were defined using the data from the previous table and divided into energy zones according to occupancy and thermal properties. Data from an in-situ energy motoring study was used to calibrate these models.

Table A1. Building archetypes in the Amsterdam urban block.

	Archetype 1	Archetype 2	Archetype 3	Archetype 4	Archetype 5	Archetype 6
Construction year	< 1975	> 1995	<1975	<1975	>1995	<1975
Building use	Domestic	Domestic	Domestic	Mixed-use	Mixed-use	Retail
Air Conditioner Use	No	Yes	No	No	Yes	Yes
R-value wall [W/m ² K]	0,35	2,5	0,35	0,35	2,5	0,35
U-value windows [W/m ² K]	5,8	1,1	5,8	5,8	1,1	5,8
Window-to-Wall Ratio	0.45	0.45	0.49	0.45	0.45	0.39
R-value roof [W/m ² K]	0,35	2,5	0,35	0,35	2,5	0,35

R-value floor [W/m ² K]	0,15	2,5	0,15	0,15	2,5	0,15
Infiltration ratio [m ³ /s per m ² façade]	0.0007	0.0004	0.0007	0.0007	0.0004	0.0007

Note. U-value indicates thermal transmittance; R-value denotes thermal resistance.

The heatwave was identified a period when the maximum daily temperature exceeds the 90th percentile for at least three consecutive days. This definition was used to select the historical heatwave year for simulation. Daily climate observations from Amsterdam Schiphol airport station for the period 1951–2023 were obtained from the NOAA (National Oceanic and Atmospheric Administration) dataset. July 23-27-2019 was identified as the heatwave with the highest maximum daily temperature (36.4°C). Figure A2 shows the hourly dry bulb temperature during the 2019 heat wave period compared to the Typical Meteorological Year (TMY). The 2019 heatwave saw temperature differences up to 15°C above the typical year, with temperatures returning to typical levels afterward.

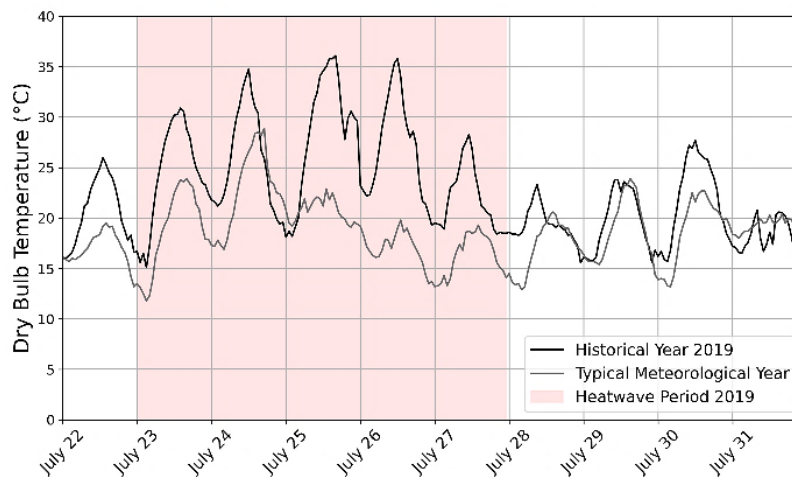


Figure A2. Amsterdam weather data..

The energy simulation results were used to derive heat resilience indicators, specifically the cumulative degree hours after the critical Standard Effective Temperature (SET) ($CDH_{SET_{crit}}$), the time to return to SET ($T_{SET_{crit}}$) and the cooling energy consumptions ($E_{Rec/Res}$), and to assess the buildings resilience score under the selected heatwave scenario (as described in deliverable D6.1). The simulation was run twice for each archetype, simulated without considering the urban context: once with natural ventilation and once with a cooling system operating from 7 AM to 7 PM, with a setpoint temperature of 25°C. An ideal loads air system, auto sized using the TMY weather data, was assumed. SET indicators were derived from the natural ventilation scenario, while energy consumption indicators came from the cooling system scenario.

A 5-day heatwave served as the reference period. $CDH_{SET_{crit}}$ measured the cumulative degree hours above SET 30°C during the heatwave, normalized by the degree hours of continuous 5°C plus the SET 30°C for the same period. E_{Res} measured cooling energy consumption during the heatwave, normalized by the end-use intensity of energy class level G which was 380 kWh/m²/year for residential buildings in the Netherlands. The RR_{Rec}

was computed considering two weeks after the heatwave as a reference period. $T_{SET_{crit}}$ normalized the hours returning to SET 30°C by the two-week recovery period. E_{Rec} normalized cooling energy consumption during recovery using the same threshold as E_{Res} , with only the reference period changing.

The final resilience score (RR_H) was calculated from the response phase due to the negligible recovery time observed after the event. This was because, following the drop in outdoor temperature immediately after the heatwave period, the indoor SET was already below 30°C when the heatwave ended. The RR_H values ranged from 0.67 to 0.77 for all the buildings (Table A2), indicating resilience ratings in classes B and A, respectively. Comparisons between archetypes revealed the influence of construction layers and shape geometry on the RR_H values. Archetypes 2 and 5 resulted in the highest RR_H values, as these buildings - constructed after 1995 - used lightweight cladding with high thermal resistance (low thermal transmittance) compared to other ones with masonry walls. For archetypes with similar E_{Res} values, E_{Res} was compared, showing that buildings with lower compactness ratios resulted in lower energy consumption.

Table A2. Heat resilience scoring per building archetype in the Amsterdam building block.

Archetype	1	2	3	4	5	6
RR_H value	0.70	0.77	0.67	0.67	0.75	0.69
Rank	3	1	5	6	2	4

Multi-hazard resilience assessment: the Acerra case study

An urban block in Acerra, Campania region (Italy), was chosen due to the area's high vulnerability to climate-induced events. The region is also potentially affected by moderate-intensity earthquakes. A multi-hazard scenario was created by considering both heat and seismic hazards. The selected area in Acerra features residential buildings with similar construction systems and materials (Table A3) but different geometries (number of stories, floor area, compactness ratio) (Figure A3).

Table A3. Building archetype in the Acerra urban block.

Construction year	Building Use	Structure		Façade		Floor	Roof
		Material	Lateral force-resisting system	Wall	Windows		
1980	Domestic	Reinforced Concrete Frame	Masonry-Infilled frames	Hollow brick masonry (R-value: 0.99 W/m2K)	Single pane, wood frame (U-value: 4.36 W/m2K)	Reinforced brick-concrete slab (R-value: 0.47 W/m2K)	Reinforced brick-concrete slab (R-value: 0.56 W/m2K)



Figure A3. Urban block analyzed in Acerra.

Table A4. Geometric characteristics per building in the Acerra urban block.

Building	1	2	3	4	5	6	7	8	9	10	11	12	13	14	15	16	17	18	19
Number of Floors	13	6	6	4	16	11	4	10	5	6	11	7	6	13	8	12	4	3	2
Total Floor Area [m ²]	5384	5742	5152	3880	8458	5784	3515	4387	2550	2954	6467	7344	5095	7801	5742	10945	977	982	112

Daily climate observations from Capodichino airport weather station for 1951–2023 were obtained from the Open-Meteo database. August 8–15-2021 was identified as the heatwave with the highest maximum daily temperature (36.9°C). Figure A4 shows the hourly dry bulb temperature during the 2021 heatwave period alongside the TMY. During the 2021 heatwave, temperatures were up to 7°C higher than the typical year. After the heatwave, temperatures for both years aligned, with values remaining above 30°C. Using this historical heatwave, an energy simulation was conducted for the 19 different buildings of the area. When calculating the RR_H values, the same indicators as the Amsterdam case study were used, with the exception of the end-use intensity of energy: class level G (Calvi et al., 2016), equating to 400 kWh/m²/year for Acerra. In this case, $CDH_{SET_{crit}}$ and $T_{SET_{crit}}$ values indicate the worst conditions for both the response and recovery periods. No clear common pattern of SET emerged between the response and recovery phases. The cooling energy consumption showed similar trends in the response and recovery phases, with higher cooling demand in the recovery phase. Building 19, with the lowest compactness ratio of 0.91, required the highest cooling demand for both the recovery and response phases. Assuming equal weight (50%) for response and recovery, the RR_H values ranged from 0.30 to 0.52 for all buildings, indicating resilience ratings in classes C, D and E. This lower resilience score, compared to the Amsterdam case study, suggests lower levels of building preparedness for extreme heat.

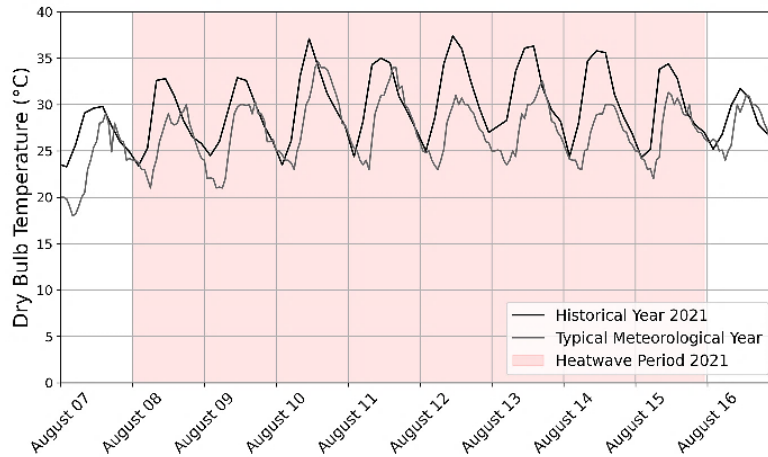


Figure A4. Acerra weather data.

The seismic resilience was assessed by means of the following indicators (see deliverable D6.1 for a full description): (i) Mean Annual Frequency of Exceedance (MAFE) relative to the collapse limit state and the expected Repair Costs to define the response phase (RR_{Res}); (ii) Downtime and Carbon Emissions for the recovery phase (RR_{Rec}). MAFE was calculated following the methodology proposed by Iervolino et al. (2018). The other indicators were assessed using the Performance-Based Earthquake Engineering (PBEE) methodology (Cornell et al., 2002), which uses hazard and vulnerability models. Hazard data was sourced from the MPS04 seismic hazard model (Stucchi et al., 2011), adjusted for B soil type. Vulnerability models specific to the Italian building stock were derived from Aljawhari et al. (2024), categorizing buildings by the number of floors and year of construction. The buildings in Acerra, constructed after the city was designated a seismic zone in 1981, were designed with some consideration of seismic actions (low-code level), though they lack the detailed seismic provisions mandated by modern codes.

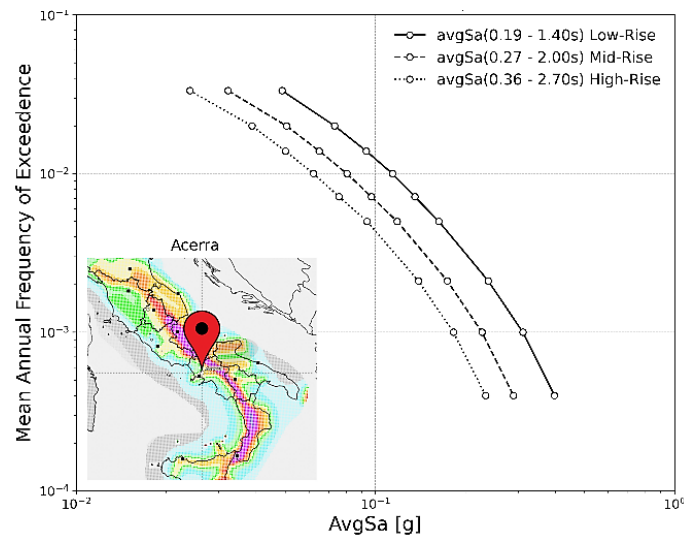


Figure A5. Seismic hazard curves (Mean Annual Frequency of Exceedance vs. Average Spectral Acceleration – AvgSa – for Low, Mid and High rise buildings).

The computed resilience indicators were normalized as indicated in deliverable D6.1. Given that the values were close to zero, they were remapped using a logistic logarithmic function for use in the MCDM approach. The mean (μ) and standard deviation (β) parameters of this function, which influence index normalization, can be defined by stakeholders to align with their risk profile and what they deem unacceptable. In this application, MAFE normalization used the minimum target (mean value of 2×10^{-4}) for new buildings as outlined by Franchin & Noto (2023), with a 0.6 dispersion value, while a 0.15% mean was applied for annual repair costs, downtime and carbon losses, with a 0.4 dispersion value. The normalized indicators for all buildings revealed that repair costs have higher impact on the response phase, resulting in a final RR_{ResE} in the range of 0.45-0.72 (using 0.5 weighting in the sub-index). In the recovery phase, normalized carbon emissions are slightly than those for downtime, leading to RR_{RecE} values between 0.28-0.67. This indicates that the buildings are better prepared for the response phase compared to the recovery phase.

The final score (C_i^*) for the building block was derived by using the $RR_{Res/Rec}$ values for heat and seismic resilience as decision criteria. The results demonstrate the influence of geometry, with taller buildings tending to have lower resilience levels. Additionally, it is observed that heat has a greater impact in the response phase, while earthquakes more significantly affect the recovery phase. This ranking provides a preliminary assessment of the area, useful for prioritizing integrated retrofitting strategies.

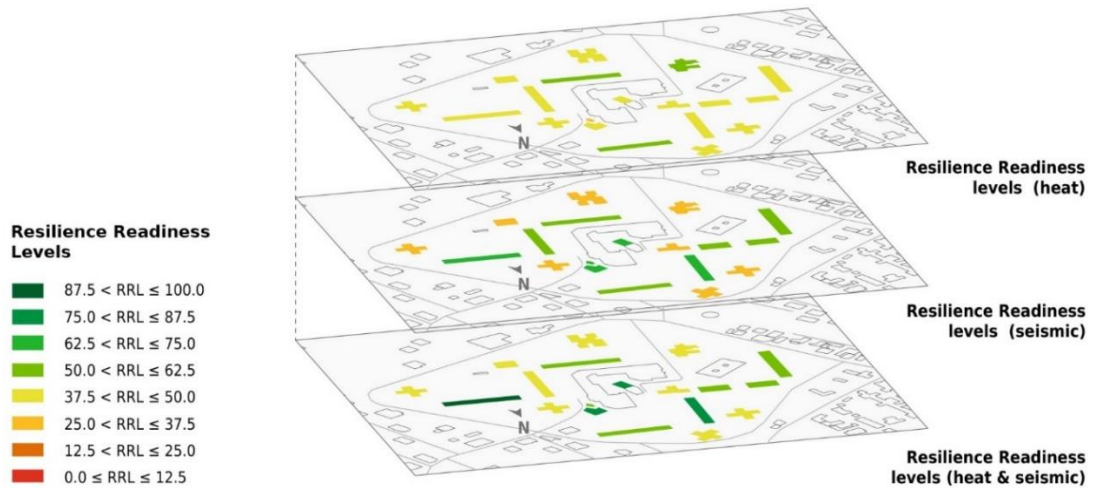


Figure A6. Resilience map for the Acerra urban block.

Table A5. Multi-hazard scoring.

Building	1	2	3	4	5	6	7	8	9	10	11	12	13	14	15	16	17	18	19
C_i^* value	0.39	0.61	0.48	0.87	0.43	0.44	0.76	0.43	0.58	0.58	0.43	0.51	0.62	0.43	0.46	0.42	0.76	0.83	0.53
RRL	D	C	D	A	D	D	A	D	C	C	D	C	C	D	D	D	A	A	C
Rank	19	6	11	1	15	13	3	16	7	8	17	10	5	14	12	18	4	2	9

References

- Calvi, G. M., Sousa, L. & Ruggeri, C. (2016) Energy efficiency and seismic resilience: A common approach. *Multi-Hazard approaches to civil infrastructure engineering*. Springer Intern. Publishing 9, 165–208.
- Iervolino, I., Spillatura, A. & Bazzurro, P. (2018) Seismic Reliability of Code-Conforming Italian Buildings. *J Earthq. Eng.* 22(sup2), 5–27.
- Cornell, C. A. & Krawinkler, H. (2000) Progress and challenges in seismic performance assessment. *PEER Center News* 3, 1-3.
- Stucchi, M., et al. (2011) Seismic Hazard Assessment (2003–2009) for the Italian Building Code. *B. Seismol. Soc. Am.* 101(4), 1885–1911.
- Aljawhari, K., Gentile, R., Galasso, C. (202) Simulation-based consequence models of seismic direct loss and repair time for archetype reinforced concrete frames. *J. Build. Eng.* 84, 108149.
- Franchin, P., Noto, F. (2023) Reliability-based partial factors for seismic design and assessment consistent with second-generation Eurocode 8. *Earth. Eng. Struct. Dyn.* 52(13), 4026-4047.